New activators of eIF2α Kinase Heme-Regulated Inhibitor (HRI) with improved biophysical properties

Qingwen Zhang, Ronghui Du, Guilherme Rodrigo Reis Monteiro dos Santos, Revital Yefidoff-Freedman, Andrew Bohm, Jose Halperin, Michael Chorev, Bertal H. Aktas

PII: S0223-5234(19)31125-0

DOI: https://doi.org/10.1016/j.ejmech.2019.111973

Reference: EJMECH 111973

To appear in: *European Journal of Medicinal Chemistry*

Received Date: 31 May 2019

Revised Date: 13 December 2019

Accepted Date: 13 December 2019

Please cite this article as: Q. Zhang, R. Du, G.R. Reis Monteiro dos Santos, R. Yefidoff-Freedman, A. Bohm, J. Halperin, M. Chorev, B.H. Aktas, New activators of eIF2α Kinase Heme-Regulated Inhibitor (HRI) with improved biophysical properties, *European Journal of Medicinal Chemistry* (2020), doi: https://doi.org/10.1016/j.ejmech.2019.111973.

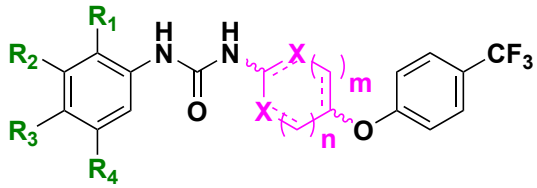

structure-activity relationship (SAR) studies

	m/n	X	Substituents on the N-phenyl				Fold stimulation of ATF-4 Surrogate eIF2α @ 1.25 µM	IC_{50}* [µM]	MW	cLogP
			R_1	R_2	R_3	R_4				
5-VI	1/1	C	H	F	CN	H	5.5	0.46	421.39	5.38
4-VI	1/1	C	H	F	H	CN	4.6	0.63	421.39	5.38

*Concentration that inhibits growth of human melanoma CRL-2813 cells by 50%

New Activators of eIF2α Kinase Heme-Regulated Inhibitor (HRI) with Improved Biophysical Properties

Qingwen Zhang [a,b #], Ronghui Du [b,c #], Guilherme Rodrigo Reis Monteiro dos Santos [b #] Revital Yefidoff-Freedman [b], Andrew Bohm [d], Jose Halperin [b], Michael Chorev [b*], and Bertal H. Aktas [b*]

[a] *Division of Medicinal and Process Chemistry, Shanghai Institute of Pharmaceutical Industry, Pudong, Shanghai 201203, China*

[b] *Hematology Laboratory for Translational Research, Department of Medicine, Brigham and Women's Hospital and Harvard Medical School, Boston, MA 02115, USA*

[c] *Medicine School of Nanjing University, Nanjing, Jiangsu 210093, China*

[d] *Tufts University Medical School, Boston, MA 02117, USA*

[#] These authors contributed equally.

* Corresponding authors

Phone: (617) 525-3142. Fax: (617) 582-6069.

E-mail: huseyin_aktas@hms.harvard.edu

Keywords:

Heme-regulated inhibitor kinase (HRI)

eIF2α phosphorylation

Cap-dependent translation

HRI activator

Drug-likeness

Cancer

Abstract

Heme-regulated inhibitor (HRI), a eukaryotic translation initiation factor 2 alpha (eIF2α) kinase, is critically important for coupling protein synthesis to heme availability in reticulocytes and adaptation to various environmental stressors in all cells. HRI modifies the severity of several hemoglobin misfolding disorders including β-thalassemia. Small molecule activators of HRI are essential for studying normal- and patho-biology of this kinase as well as for the treatment of various human disorders for which activation of HRI or phosphorylation of eIF2α may be beneficial. We previously reported development of 1-((1,4-*trans*)-4-aryloxycyclohexyl)-3-arylureas (cHAUs) as specific HRI activators and demonstrated their potential as molecular probes for studying HRI biology and as lead compounds for treatment of various human disorders. To develop more druglike cHAUs for *in vivo* studies and drug development and to expand the chemical space, we undertook bioassay guided structure–activity relationship studies replacing cyclohexyl ring with various 4-6-membered rings and explored further substitutions on the *N*-phenyl ring. We tested all analogs in the surrogate eIF2α phosphorylation and cell proliferation assays, and a subset of analogs in secondary mechanistic assays that included endogenous eIF2α phosphorylation and expression of C/EBP homologous protein (CHOP), a downstream effector. Finally, we tested specificity of these compounds for HRI by testing their anti-proliferative activity in cells transfected with siRNA targeting HRI or mock. These compounds have significantly improved cLogPs with no loss of potencies, making them excellent

candidates for lead optimization for development of investigational new drugs that potently and specifically activate HRI.

Abbreviations:

ΦO*c*HΦUs, 1-phenyl-3-(4-phenoxy)cyclohexyl)ureas; ΦO*c*AlkΦUs, 1-phenyl-3-(4-phenoxy)cycloalkyl)ureas; 4-CF_3-ΦO*c*AlkΦUs, 1-phenyl-3-((1,3/4-*trans*)-4-(4-trifluoromethyl)phenoxy)cycloalkyl)ureas; 4-CF_3-ΦO*c*BΦUs, 1-phenyl-3-((1,3-*trans*)-4-(4-trifluoromethyl)phenoxy)cyclobutyl)ureas; 4-CF_3-ΦO*c*PΦUs, 1-phenyl-3-((1,3-*trans*)-4-(4-trifluoromethyl)phenoxy)cyclopentyl)ureas; 4-CF_3-ΦO*c*HΦUs, 1-phenyl-3-((1,4-*trans*)-4-(4-trifluoromethyl)phenoxy)cyclohexyl)ureas; 4-CF_3-ΦOPyΦUs, 1-phenyl-3-(5-(4-(trifluoromethyl)phenoxy)pyrimidin-2-yl)ureas; HRI, heme regulated inhibitor or heme regulated eIF2α kinase; eIF2, eukaryotic translation initiation factor 2; eIF2α, eukaryotic translation initiation factor 2 alpha; GTP, guanosine triphosphate; Met-$tRNA_i$, initiator methionyl tRNA; mRNA, messenger RNA; ATF-4, activating transcription factor 4; CHOP, C/EBP homology protein; PPAR−γ, peroxisome proliferator-activated receptor γ; SAR, structure-activity relationship; LC-MS, liquid chromatography-mass spectrometry; NMR, nuclear magnetic resonance; DIAD, diisopropyl azodicarboxylate; TFA, trifluoroacetic acid; BOC, *tert*-butyloxycarbonyl; DMF, *N*,*N*-dimethylformamide; NMP, *N*-methyl-2-pyrrolidinone; DMSO, dimethyl sulfoxide; DRL assay, surrogate dual-luciferase eIF2α phosphorylation assay; uORFs, upstream open reading frames; 5'UTR, 5' untranslated region; Cycloalk. config., Cycloalkyl configuration.

1. Introduction

Eukaryotic translation initiation factor 2 alpha (eIF2α) kinases play critical roles in responding to various stress conditions and adapting cellular metabolism to extracellular cues. Heme regulated eIF2α kinase, also known as heme regulated inhibitor (HRI), was first of four eIF2α kinases to be discovered. HRI expression is highest in the red blood cell (RBC) precursors where it critically contributes to differentiation and maturation of myelogenic lineage into RBCs. In the RBC precursors, HRI is maintained in the inactive state by heme [1]. Low levels of free heme lead to HRI activation through

autophosphorylation [2]. Activated HRI phosphorylates eIF2α, which reduces the level of the translation initiation complex formed by eIF2, GTP and Met-tRNA$_i$ (the ternary complex, eIF2·GTP·Met-tRNA$_i$), which is critical for the formation of the 43S pre-initiation complex [3]. Reducing the amount of the ternary complex inhibits translation initiation thereby reducing global protein synthesis. By coupling globin synthesis to heme availability, HRI plays a critical role in attenuating severity of iron-deficiency anemia, β-thalassemia and most likely other anemic disorders [4].

HRI expression is not limited to myelogenic lineage; it is expressed in almost all tissues examined. HRI is the only eIF2α kinase activated by arsenate induced oxidative stress [5]. It is also activated by nitrous oxide [6], osmotic shock, and heat shock [7]. By phosphorylating eIF2α and reducing the amount of the ternary complex, HRI activates downstream effectors of this pathway including activating transcription factor 4 (ATF-4) and pro-apoptotic transcription factor C/EBP homology protein (CHOP). Activation of HRI (and the resulting phosphorylation of eIF2α) may initially be cytoprotective but its sustained activation may cause cell death [8].

Recent discovery of small molecule activators of HRI [9-12] provided scientific community with tools to better understand the role of this kinase as well as eIF2α phosphorylation in normal- and patho-biology. For example, these agents allowed us and others to study HRI's regulation of fibroblast growth factor 21 (FGF21) activity and its role in diabetes and fatty liver disease and interaction of HRI/eIF2α-P/ATF-4 pathway with the PPAR-γ pathway [13,14], regulation of host/intracellular pathogen interactions

[15,16], and treatment of therapy resistant multiple myeloma cancers [8,17]. Importantly, when employed in combination with other eIF2α kinase activators, HRI activators are invaluable tools for dissecting contribution of eIF2α vs other substrates of eIF2α kinases to normal- and patho-biology. This cannot be accomplished by using non-specific eIF2α activators or eIF2α phosphatase inhibitors [18,19]. Understanding the molecular basis of HRI activation by small molecules will be helpful for better understanding diverse roles heme and heme regulated proteins in normal- and patho-physiology [20].

Demonstration by us others that modulation of eIF2α phosphorylation is a viable approach for the treatment of animal models of proliferative and some neurodegenerative disorders [18,19,21-24] prompted us to further screen libraries of small molecules to identify inducers of eIF2α phosphorylation. Initially, we screened a diverse *N*,*N*'-disubstituted urea library, discovered 1-phenyl-3-(4-phenoxy)cyclohexyl)ureas (ΦO*c*HΦUs) as potent *in vitro* inducers of HRI-dependent phosphorylation and carried out a limited structure-activity relationship (SAR) study [11]. Subsequently, design and synthesis of focused library of ΦO*c*HΦUs led us to novel druglike analogs with improved biophysical properties that potently induce eIF2α phosphorylation and expression of its downstream effector CHOP and inhibit cancer cell proliferation at sub-micromolar concentrations [12]. Moreover, one of the ΦOcHΦUs with more potent *in vitro* activity (1-(3-cyano-5-trifluoromethyl)phenyl-3-(*trans*-4-(4-(trifluoromethyl)phenoxy)cyclohexyl) urea, **1-VI** in Table 1) displayed *in vivo* efficacy in xenograft mice model of human melanoma with no apparent organ toxicity and a very encouraging target validation

profile. To better delineate the pharmacophore in the ΦO*c*HΦUs and further optimize the biophysical properties to improve bioavailability and develop a promising lead candidate for a comprehensive preclinical development, we undertook a new round of SAR optimization. To this end, our study focuses on the cyclohexyl linker scaffolding the phenoxy and the *N*-phenyl ureido moieties in the ΦO*c*HΦU chemotype. Herein we report on novel more druglike ΦO*c*HΦUs that activate eIF2α phosphorylation and its downstream effectors, and potently inhibit cancer cells proliferation. With this information in hand we believe to have promising molecular probes and candidates for comprehensive *in vivo* preclinical evaluation aimed at understanding the role of HRI and eIF2α phosphorylation in normal- and patho-biology. These studies could help the advancement of HRI activators as mechanistically unique agents for treatment of human disorders.

2. Results and discussion

2.1. Molecular design

Recently we reported progress in optimizing the ΦO*c*HΦU chemotype in which a combination of *N*-(3-trifluoromethyl-5-cyano)phenyl and *N*-(1,4-*trans*)-(4-(4-trifluoromethyl)phenoxy)cyclohexyl) moieties contributes to enhanced potency and more favorable cLogP values [12]. Herein we designed focused libraries of *N,N'*-disubstituted ureas to examine the role of the *N*-(1,4-*trans*)-cyclohexyl moiety as a locally constraining linker by replacing it with cyclopentyl and cyclobutyl that are smaller, less hydrophobic and more constrained cycloalkyl moieties. In addition, we also sought to test the hypothesis that global constraint introduced by replacing the

(1,4-*trans*)-cyclohexyl with a 2,5-pyrimidyl may form a 6-membered hydrogen bond with the distant ureido NH. Furthermore, we were eager to explore the impact of nature and position of the *N*-phenyl substituents on HRI activity and drug-likeness of the desired *N,N'*-disubstituted ureas.

2.*2. Synthesis*

The common and principal intermediates for the synthesis of this series of 1-phenyl-3-(4-phenoxy)cycloalkyl)ureas (ΦO*c*AlkΦUs) are the 3/4-(4-(trifluoromethyl)phenoxy)cycloalkan-1-amines (**B**) (Scheme 1). Based on the commercial availability of starting materials the synthesis of **B** was accomplished by 2 different approaches: 1. Mitsunobu coupling of a variety of *tert*-butyl (3/4-hydroxycycloalkyl)carbamates with 4-(trifluoromethyl)phenol in the presence of triphenylphosphine and diisopropyl azodicarboxylate (DIAD) in anhydrous THF delivered the Mitsunobu products *tert*-butyl (3/4-(4-(trifluoromethyl)phenoxy)cycloalkyl)carbamates (**A**). Treatment of **A** with trifluoroacetic acid (TFA) removed the protecting group BOC (*tert*-butyloxycarbonyl) and yielded the amines **B** in good yields (Pathway AI) [25]. The Mitsunobu reaction provides a highly reliable method to inverting the configuration of secondary alcohol chiral carbon [26]. **A**-**V** was prepared from optically pure *tert*-butyl (1*S*,3*R*)-3-hydroxycyclopentyl carbamate (**C,** m=0, n=1). We have successfully harvested from methylene chloride single crystals of **A**-**V**, whose absolute configuration was determined to be (*1S,3S*) by single crystal X-ray diffraction (Cambridge Crystallographic Data Centre 1871144) (Fig. 1). As anticipated, this result confirms the inversion of configuration of the chiral center

undergoing the Mitsunobu reaction. 2. A direct *O*-alkylation of (1,4-*trans*)-4-aminocyclohexan-1-ol by 1-fluoro-4-(trifluoromethyl)benzene in the presence of NaH in DMF furnished the known intermediate **B** (m=1, n=1) (Pathway AII) [11,12].

With this common and principal intermediate **B** in hand, the desired *N,N'*-disubstituted ureas were readily accessed by acylation with either commercially available isocyanates **D** (Pathway A) or substituted phenyl carbamates **E** that were conveniently prepared from the corresponding anilines **F** and phenyl chloroformate (Pathway B) (Scheme 1).

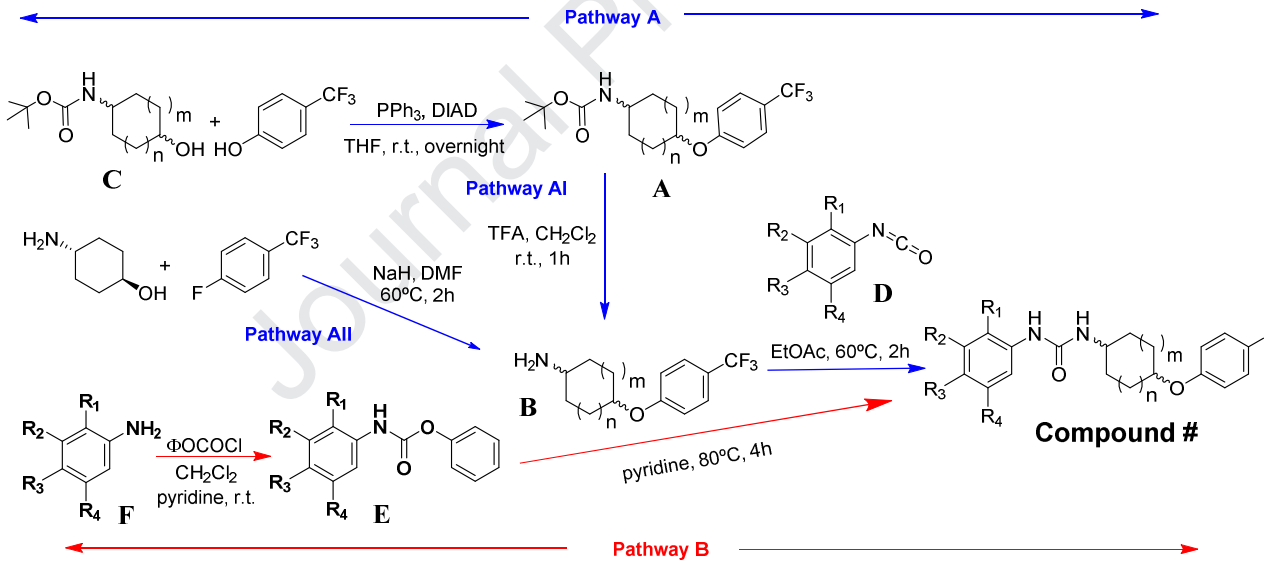

1-phenyl-3-(3-(4-(trifluoromethyl)phenoxy)cycloalkyl)ureas

Comp. #	Pathway	Cycloalk. config.	m	n	R_1	R_2	R_3	R_4
1-VI [12]	B	1,4-*trans*	1	1	H	CF_3	H	CN
1-V	B	1S,3S	0	1	H	CF_3	H	CN
1-IV	B	1,3-*trans*	0	0	H	CF_3	H	CN
1-IV*c*	B	1,3-*cis*	0	0	H	CF_3	H	CN
2-VI [11]	AII	1,4-*trans*	1	1	H	CF_3	H	H
2-V	AI	1S,3S	0	1	H	CF_3	H	H
2-IV	AI	1,3-*trans*	0	0	H	CF_3	H	H
2-IV*c*	AI	1,3-*cis*	0	0	H	CF_3	H	H
3-VI [12]	AII	1,4-*trans*	1	1	H	CN	H	H
3-V	AI	1S,3S	0	1	H	CN	H	H
3-IV	AI	1,3-*trans*	0	0	H	CN	H	H
3-IV*c*	AI	1,3-cis	0	0	H	CN	H	H
4-VI	AII	1,4-*trans*	1	1	H	F	H	CN
4-V	AI	1S,3S	0	1	H	F	H	CN
4-IV	AI	1,4-*trans*	0	0	H	F	H	CN
5-VI	B	1,4-*trans*	1	1	H	F	CN	H
6-VI	B	1,4-*trans*	1	1	F	H	H	CN
7-VI	AII	1,4-*trans*	1	1	CH_3	H	H	F
7-V	AI	1S,3S	0	1	CH_3	H	H	F
7-IV	AI	1,3-*trans*	0	0	CH_3	H	H	F
8-VI	B	1,4-*trans*	1	1	F	H	CN	H
9-VI	B	1,4-*trans*	1	1	H	CN	F	H
10-VI	AII	1,4-*trans*	1	1	H	F	F	H
10-V	AI	1S,3S	0	1	H	F	F	H
10-IV	AI	1,3-*trans*	0	0	H	F	F	H
11-VI	AII	1,4-*trans*	1	1	F	F	H	H
11-IV	AI	1,3-*trans*	0	0	F	F	H	H

Scheme 1. Synthetic pathways employed for the synthesis of 1-phenyl-3-(3/4-(4-(trifluoromethyl)phenoxy)cycloalkyl)ureas (4-CF_3-ΦO*c*AlkΦUs). Pathway A generated the desired *N,N'*-disubstituted ureas utilizing isocyanates to acylate the substituted cycloalkylamine **B**. The later was generated through either a Mitsunobu coupling of BOC protected aminocycloalkanol **C** (m=0, n=1 for cyclopentyl series; m=0, n=0 for cyclobutyl series) and 4-(trifluoromethyl)phenol followed by TFA deprotection (Pathway AI) or *O*-alkylation of (1,4-*trans*)-4-aminocyclohexan-1-ol (m=1, n=1 for cyclohexyl series) by 1-fluoro-4-(trifluoromethyl)benzene (Pathway AII). Pathway B employed phenyl carbamates **E** as acylating agents of the *O*-substituted 3/4-hydroxycycloalkan-1-amines **B**. The phenyl carbamates **E** were obtained by acylating substituted anilines **F** with phenyl chloroformate.

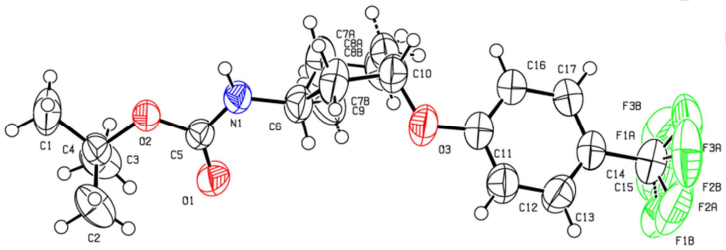

Fig. 1. X-ray ORTEP diagram of **A-V**.

The synthesis of this series of 1-phenyl-3-(5-(4-(trifluoromethyl)phenoxy)pyrimidin-2-yl)ureas (4-CF_3-ΦOPyΦUs: **1-py** – **4-py**, **7-py** and **10-py**) utilized Pathways AII and B (Scheme 2). The initial attempted condensation of 5-chloropyrimidin-2-amine and 4-(trifluoromethyl)phenol in the presence of potassium hydroxide and potassium carbonate at elevated temperature in DMF or NMP failed to deliver the key intermediate 5-(4-(trifluoromethyl)phenoxy)pyrimidin-2-amine (G). Alternatively, 2-aminopyrimidin-5-ol was condensed with 1-fluoro-4-(trifluoromethyl)benzene. Due to the greater acidity of 2-aminopyrimidin-5-ol *vs* (1,4-*trans*)-4-aminocyclohexan-1-ol, NaH/DMF used for the formation of (1,4-*trans*)-4-(4-(trifluoromethyl)phenoxy)cyclohexan-1-amine (**B**, m=1, n=1) was replaced

with Cs_2CO_3/DMSO for the formation of the key intermediate G albeit at lower yields (Scheme 2).

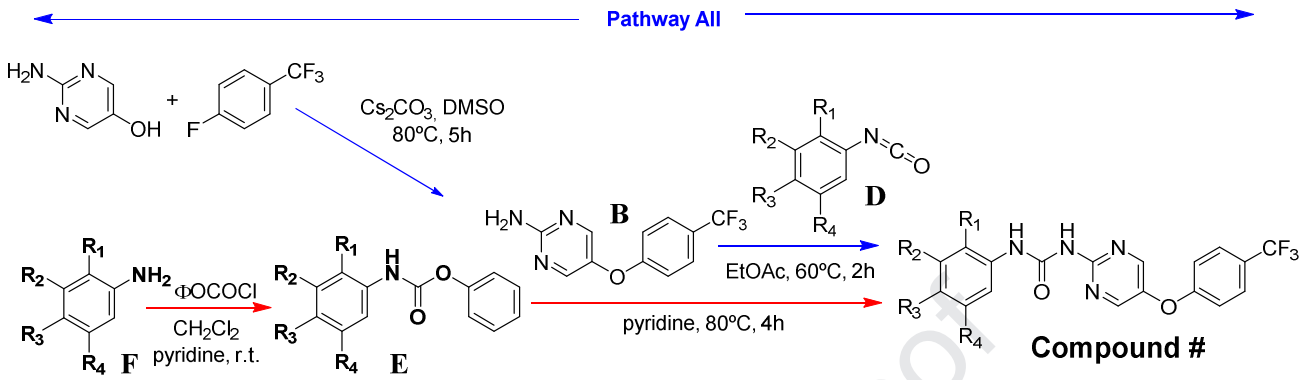

1-phenyl-3-(5-(4-(trifluoromethyl)phenoxy)pyrimidin-2-yl)ureas

Comp #	Pathway	R_1	R_2	R_3	R_4
1-py	AII	H	CF_3	H	CN
2-py	AII	H	CF_3	H	H
3-py	B	H	CN	H	H
4-py	B	H	F	H	CN
7-py	AII	CH_3	H	H	F
10-py	AII	H	F	F	H

Scheme 2. Synthetic pathways employed for the synthesis of 1-phenyl-3-(5-(4-(trifluoromethyl)phenoxy)pyrimidin-2-yl)urea series (4-CF_3-ΦOPyΦUs). Pathway A delivered the desired *N*,*N*'-disubstituted ureas utilizing isocyanates to acylate the key intermediate G, 5-(4-(trifluoromethyl)phenoxy)pyrimidin-2-amine. The later was generated through *O*-arylation of 2-aminopyrimidin-5-ol by 1-fluoro-4-(trifluoromethyl)benzene in the presence of cesium carbonate in DMSO (Pathway AII). Pathway B employed phenyl carbamates **E** as acylating agents of the key intermediate G. The phenyl carbamates **E** were obtained by acylating substituted anilines **F** with phenyl chloroformate.

It's advisable to replace B with G in Scheme 2 to avoid confusion.

On the basis of analytical reverse-phase high-performance liquid chromatography (RP-HPLC) analysis, the purity of all final *N*,*N*'-disubstituted ureas submitted to biological characterization and reported herein equaled or exceeded 95%. Their structural identity and integrity were confirmed by LC−MS as well as ^{1}H-, ^{13}C-, and ^{19}F-NMR.

2.3. Biological Results and Discussion

Structure-activity relationship studies. All newly synthesized *N,N*'-disubstituted ureas were initially evaluated by testing them in the surrogate eIF2α phosphorylation dual-luciferase reporter (DLR) assay [9,27]. Briefly, this assay takes advantage of the fact that activated HRI phosphorylates eIF2α which inhibits eIF2 guanine nucleotide exchange factor eIF2B, responsible for exchanging the GDP in the eIF2.GDP complex for GTP. The reduction in the recycling of eIF2.GDP into eIF2.GTP interferes with the formation of eIF2·GTP·Met-tRNA$_i$ ternary complex. This results in the inhibition of overall translation, but paradoxically, increases translation of a small subset of mRNAs that contain multiple upstream open reading frames (uORFs) in their 5' untranslated region (5'UTR). These include mRNA coding for activating transcription factor 4 (ATF-4) [18,19,28]. In our assay, firefly (F) luciferase ORF is fused to the 5'UTR of ATF-4 mRNA that has multiple uORFs while renilla (R) luciferase ORF is fused to a 5'UTR lacking any uORFs. Agents that reduce the amount of the eIF2·GTP·Met-tRNA$_i$ ternary complex, such as those *N,N*'-disubstituted ureas that activate HRI, increase F luciferase expression while reducing the R luciferase expression, resulting in an increased F/R luciferase ratio. The newly synthesized ureas were tested at 10, 5, 2.5, and 1.25 μM concentrations in 96-well assay plates [9,29]. We calculated the activity scores as the F/R ratios for every compound-treated well and normalized these to F/R ratio of vehicle-treated (DMSO) wells in the same plate, arbitrarily set at 1 (F/R = 1). Data obtained in the surrogate dual-luciferase eIF2α phosphorylation (DLR) assay for the series of

1-phenyl-3/4-(4-trifluorometyl)phenoxy-cycloalkyl)ureas (4-CF_3-ΦO*c*AlkΦUs) and 1-phenyl-3-(5-(4-(trifluoromethyl)phenoxy)pyrimidin-2-yl)ureas (4-CF_3-ΦOPyΦUs) reported herein are shown in respective Tables 1 and 2.

Table 1 (Uploaded separately)

Table 2

Substitution pattern and cLogP of the 1-phenyl-3-(5-(4-(trifluoromethyl)phenoxy-pyrimidin-2-yl)ureas ((4-CF_3)ΦOPyrΦUs)*

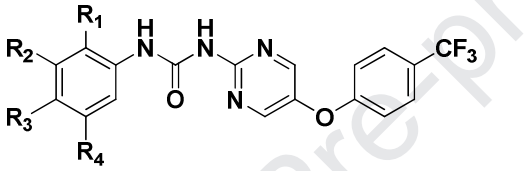

	R_1	R_2	R_3	R_4	cLogP
1-py	H	CF_3	H	CN	5.27
2-py	H	CF_3	H	H	5.80
3-py	H	CN	H	H	4.37
4-py	H	F	H	CN	4.52
7-py	CH_3	H	H	F	4.97
10-py	H	F	F	H	5.12

*No activity in the surrogate dual-luciferase eIF2α phosphorylation assay up to 20 μM.

In our previous reports we have identified two 1-phenyl-3-((1, 4-*trans*)-4-(4-trifluorometyl)phenoxy)cyclohexyl)ureas (4-CF_3-ΦO*c*HΦUs) **1-VI** and **2-VI** as promising leads [11,12]. Both have a (4-trifluoromethyl)phenoxy ring and while **2-VI** has a *N*-(3-trifluoromethyl)phenyl **1-VI** carries the *N*-(3-trifluormethyl-5-cyano)phenyl moiety leading to slightly different cLogP (6.41 and 6.20, respectively). Accordingly, both activate HRI though **1-VI** is more active (3.6- and 5.7-fold increase in the surrogate eIF2α phosphorylation assay at 1.25μM for **2-VI** and **1-VI**, respectively). The subsequent

focused library of 4-CF_3-ΦO*c*HΦUs reported herein was prepared to reduce hydrophobicity without compromising potency. All include a (4-trifluoromethyl)phenoxy moiety and differ in nature and position of the substituents on the *N*-phenyl moiety. The most potent analog in this library, **5-VI**, is almost equipotent with **1-VI** (5.5- and 5.7-fold increase at 1.25 μM, respectively) but has significantly lower cLogP than the latter (cLogP=5.38 vs 6.20, respectively). Moreover, the 2,3-difluorophenyl carrying 4-CF_3-ΦO*c*HΦU **11-VI** has potency that falls in between the two earlier leads, **1-VI** and **2-VI,** but it is somewhat less hydrophobic than **5-VI** (cLogP=5.17 vs 5.38, respectively). Evidently, replacement of the hydrophobic CF_3 substituent in **1-VI** with F, a smaller and less hydrophobic substituent (cf. **1-VI** with **5-VI**) results in an insignificant loss in potency but a significant reduction in hydrophobicity. Interestingly, the least hydrophobic 4-CF_3-ΦO*c*HΦUs in this series **6-VI** and **8-VI**, presenting two polar and electron withdrawing substituents as either *N*-(2-fluoro-5-cyano)phenyl or *N*-(2-fluoro-4-cyano)phenyl, respectively, are not among the most potent analogs. We suspect that the nature of substituents and their positions on the *N*-phenyl ring are more important for high potency than the overall hydrophobicity.

Interestingly, in the 4-CF_3-ΦO*c*BΦUs series we have 3 pairs of *cis* and *trans* isomers **1-IV** and **1-IV*c***, **2-IV** and **2-IV*c*** and **3-IV** and **3-IV*c*** listed in the decreasing order of potency but almost equipotent within the pairs (e.g causing 4.4- and 4.3-fold increase in the F/R ratio in the surrogate eIF2α phosphorylation assay at 1.25 μM for **1-IV** and **1- IV*c*,** respectively, and IC_{50} of 0.9 μM for both *vs* increasing F/R ratio 1.6- and 1.1-fold at 1.25

μM and IC_{50}=4.9 and >10 μM for **3-IV** and **3-IV*c*,** respectively) (Table 1)**.** In line with this observation, the greater commercial availability of (1,4-*trans*)-4-aminocyclohexan-1-ol and its greater metabolic stability [30] we select the *trans* isomer as preferential leads for further preclinical development.

Our working hypothesis is that the cycohexyl moiety in the ΦO*c*HΦU series serves as a scaffold to link between the two parts of the pharmacophore, the *N*-phenyl substituted urea moiety and the substituted phenoxy moiety. As such, reducing the size of the cycloalkyl linker will reduce the overall hydrophobicity and at the same time will also affect the overall rigidity of the *N*-aryl urea. With that in mind we generated two focused libraries of 1-phenyl-3-((1,3-*trans*)-4-(4-trifluorometyl)phenoxy)cyclopentyl)ureas (4-CF_3-ΦO*c*PΦUs) and 1-phenyl-3-((1,3-*trans*)-4-(4-trifluorometyl)phenoxy)cyclobutyl)ureas (4-CF_3-ΦO*c*BΦUs). Indeed, reducing the ring size of the cycloalkyl moiety was accompanied by a consistent lowering of cLogP (e.g. 6.41, 6.29, 6.16 for the 4-CF_3-ΦO*c*HΦU – **2-VI**, 4-CF_3-ΦO*c*PΦU – **2-V** and 4-CF_3-ΦO*c*BΦU – **2-IV**, respectively). Remarkably, none of the analogs incorporating either the cyclobutyl or the cyclopentyl moieties were more potent or even equipotent to the corresponding cyclohexyl containing analog. Possibly, the conformational rigidification accompanying reduction in ring size and/or compromise of critical hydrophobic interactions enabled by the cyclohexyl ring prevent both the 4-CF_3-ΦO*c*PΦUs and the 4-CF_3-ΦO*c*BΦUs from achieving the same effective target complementing interactions provided by the 4-CF_3-ΦO*c*HΦUs.

Replacement of the (1,4-*trans*)-4-(4-trifluoromethyl)phenoxycyclohexyl moiety in 4-CF_3-ΦO*c*HΦUs with 5-(4-trifluoromethyl)phenoxy)pyrimidin-2-yl as in 4-CF_3-ΦOPyΦUs aimed in addition to testing another mode of reducing hydrophobicity this time by replacing the 1,4-disubstituted cyclohexyl with 2,5-disubstituted pyrimid-2-yl (cf. e.g. cLogP of **2-VI** and **2-py** 6.41 and 5.80, respectively) also testing for an interesting mode of global molecular rigidification. This rigidification involves the replacement of the flexible puckering cyclohexyl ring with the aromatic planar pyrimidyl ring and enablement of the formation of a planar conjugated pseudo six-membered ring generated by an intramolecular hydrogen bond within the pyrimidin-2-yl-urea motif (denoted in red in Scheme 3), which was calculated to be more stable than the extended conformation [31,32]. Nevertheless, due to the pairing of one hydrogen bond donor and one hydrogen bond acceptor to pseudo six-membered ring these H-donor and -acceptors are no longer available for intermolecular interactions with water and therefore aqueous solubility was lower than the one anticipated from compounds of the same cLogP that do not form intramolecular hydrogen bonds [33]. All the compounds within the focused library of 4-CF_3-ΦOPyΦUs were devoid of activity in the surrogate eIF2α phosphorylation assay even up to 20 μM as measured in the DLR assay. We suspect that this mode of molecular rigidification may lock compounds in an orientation that could not accommodate the HRI activation and therefore did not lead to the activity in the surrogate eIF2α phosphorylation assay.

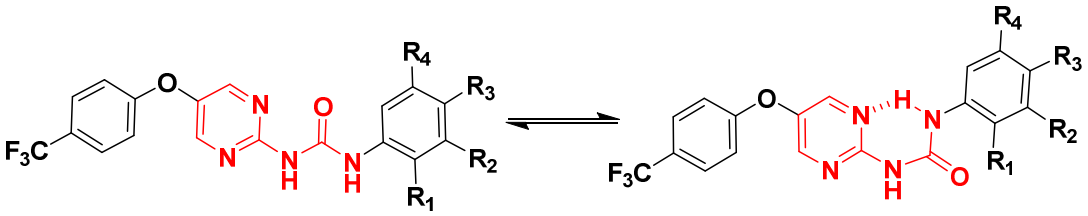

Scheme 3. Potential molecular rigidification by a putative planar pseudo six-membered ring generated by an intramolecular hydrogen bond within the pyrimidin-2-yl-urea motif

Biological activities in secondary mechanistic assays. To validate the newly synthesized 4-CF_3-ΦO*c*AlkΦUs and 4-CF_3-ΦOPyΦUs as activators of HRI, and thereby inducers of eIF2α phosphorylation, we selected most of the 4-CF_3-ΦO*c*HΦUs (**4-VI**, **5-VI**, **6-VI**, **7-VI**, **11-VI** and **1-VI**) and the most potent 4-CF_3-ΦO*c*BΦU (**1-IV**) (Table 1) and tested them in the secondary mechanistic assays that included phosphorylation of endogenous eIF2α and expression of its downstream effector CHOP.

Endogenous eIF2α is the best-known substrate of HRI and the upstream regulator of the eIF2·GTP·Met-tRNA$_i$ ternary complex abundance, while CHOP expression is a downstream effector of eIF2α phosphorylation. For assessing eIF2α phosphorylation we blotted cell lysates treated for two hours with vehicle or selected compounds using antibodies specific for the total-eIF2α and the phosphorylated-eIF2α (T-eIF2α and [PhoS^{51}]-eIF2α), respectively. [34] (Figure 2A). The least potent analog **6-VI** in stimulating eIF2α phosphorylation as measured by the surrogate eIF2α phosphorylation assay was also the least active one in phosphorylating endogenous eIF2α in adherent human melanoma CRL-2813 cells as determined by Western blot analysis. Moreover, in CRL-2813 cells treated with the *N*,*N*'-disubstituted ureas for eight hours, expression of CHOP protein as well as expression of cell cycle regulatory proteins, the oncogenic protein cyclin D1 and the cyclin dependent kinase (CDK) inhibitor p27^{Kip1} that prevents activation of cyclin/CDK complexed at the G1 phase of cell cycle, was very revealing. As anticipated, relative to DMSO, the control vehicle, active 4-CF_3-ΦO*c*HΦUs (**1-VI**, **4-VI**, **5-VI**, **7-VI** and **11-VI**) and 4-CF_3-ΦO*c*BΦUs (**1-IV**) increased the expression of CHOP, a

downstream effector of eIF2α phosphorylation, and decreased the expression of cyclin D1 whose expression is dependent on the abundance of the ternary complex [28,29] (Fig. 2B). Consistently, 4-CF_3-ΦO*c*HΦU **6-VI,** which was inactive in the DLR assay, neither increased expression of CHOP and nor inhibited the expression of cyclin D1 [28,35] (Fig. 2B). As anticipated, none of the analogs affected the expression of housekeeping proteins such as $p27^{Kip1}$ and β-actin (Fig. 2B).

In summary, the results obtained with the secondary and tertiary mechanistic assays reported herein are in full agreement with the data from the surrogate eIF2α phosphorylation reporter assay and thus support our conclusion that our active 4-CF_3-ΦO*c*AlkΦUs are targeting the ternary complex by activating HRI.

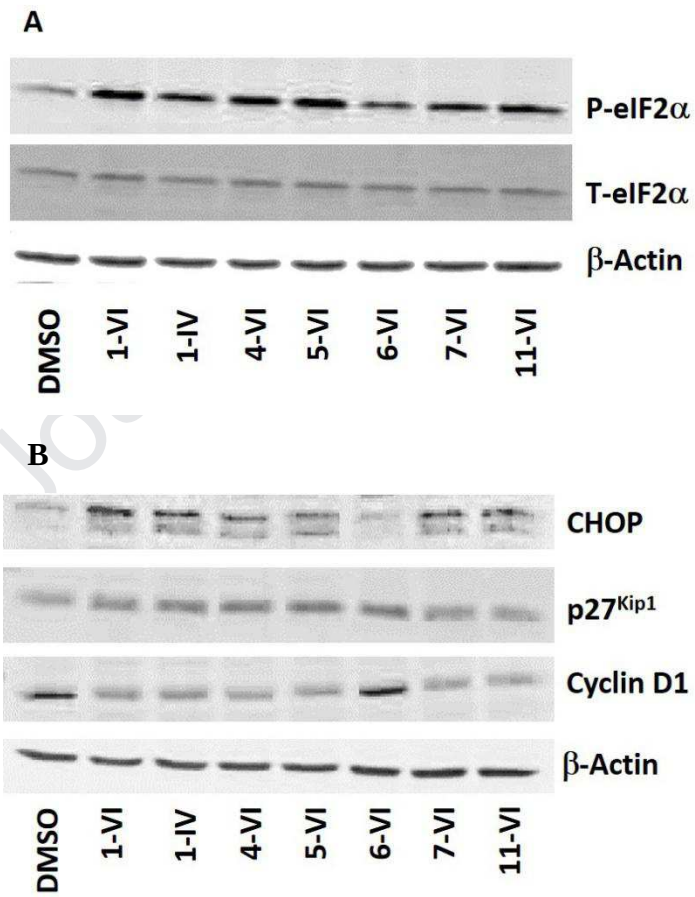

Fig. 2. HRI activators induce eIF2α phosphorylation and modify its downstream effectors. A. CRL-2813 cells were treated with 5 μM of each compound for 2 hours, cell

lysates were probed with phosphorylated (P-eIF2α) and total eIF2α (T-eIF2α) and β-actin specific antibodies. **B**. CRL-2813 cells were treated with 5 μM HRI activators for 8 hours and lysates were immunoblotted with antibodies against CHOP, $p27^{Kip1}$, cyclin D1 and β-actin (Also uploaded separately as a TIFF Figure).

In vitro **cell proliferation studies**. All 4-CF_3-ΦO*c*AlkΦUs were tested in the sulforhodamine B (SRB) cell proliferation assay to establish the concentrations that inhibit human melanoma CRL-2813 cells growth by 50% (IC_{50}) (Table 1). This activity reflects a combined effect of membrane permeability and overall anti-proliferative effects that include on target as well as off-target effects. Therefore, by correlating the IC_{50}s with the activity of the compounds in the surrogate dual-luciferase eIF2α phosphorylation reporter (DLR) assay we may gain valuable insight into compounds' specificity and mode of action (Table 1). Evidently, the most active analogs that are part of the 4-CF_3-ΦO*c*AlkylΦU series display IC_{50}s in the sub-micromolar range (e.g. 0.46 and 0.9 μM for **5-VI** and **1-IV**, respectively). Moreover, there is a very good correlation between the activity of the compounds in the surrogate eIF2α phosphorylation reporter assay and the IC_{50} values in the cell proliferation assay (e.g. 5.7-, 3.1- and 4.4-fold at 1.25 μM and 13.8-, 8.3- and 10-fold at 5 μM in the surrogate eIF2α-P assay vs IC_{50}s of 0.35, 1.2 and 0.9 μM, for respective **1-VI**, **1-V** and **1-IV**) (Table 1). Together, these results strongly support our hypothesis that anti-proliferative activity of 4-CF_3-ΦO*c*AlkylΦUs analogs is primarily contributed through the activation of HRI. This is consistent with our previously

reported 4-CF_3-ΦO*c*HΦUs **1-VI**, **2-VI** and **3-VI** that inhibit cell proliferation by activating HRI and inducing eIF2α phosphorylation [9-12].

Specificity of HRI activators. To determine the specificity of our newly synthesized lead compounds for HRI we knockdown expression of HRI in MCF-7 cells using a pool of siRNA targeting HRI and used cell proliferation assay as a biologic response parameter [9,11]. We choose this assay because it compares specificity of the compounds for HRI compared to all other cellular targets that can impinge on cell proliferation. We treated MCF-7 human breast cancer cells transfected with siRNA targeting HRI or vehicle with various concentrations of 4-CF_3-ΦO*c*HΦUs (**1-VI**, **4-VI**, and **5-VI**) and 4-CF_3-ΦO*c*BΦU (**1-IV**). MCF-7 cells were chosen because knockdown efficiency in these cells is significantly higher than in CRL-2813 cells [9]. As shown in Figure 3 knocking down HRI expression caused a dramatic reduction in the activity of all four compounds tested. These data demonstrate that 4-CF_3-ΦO*c*HΦUs specifically activate HRI.

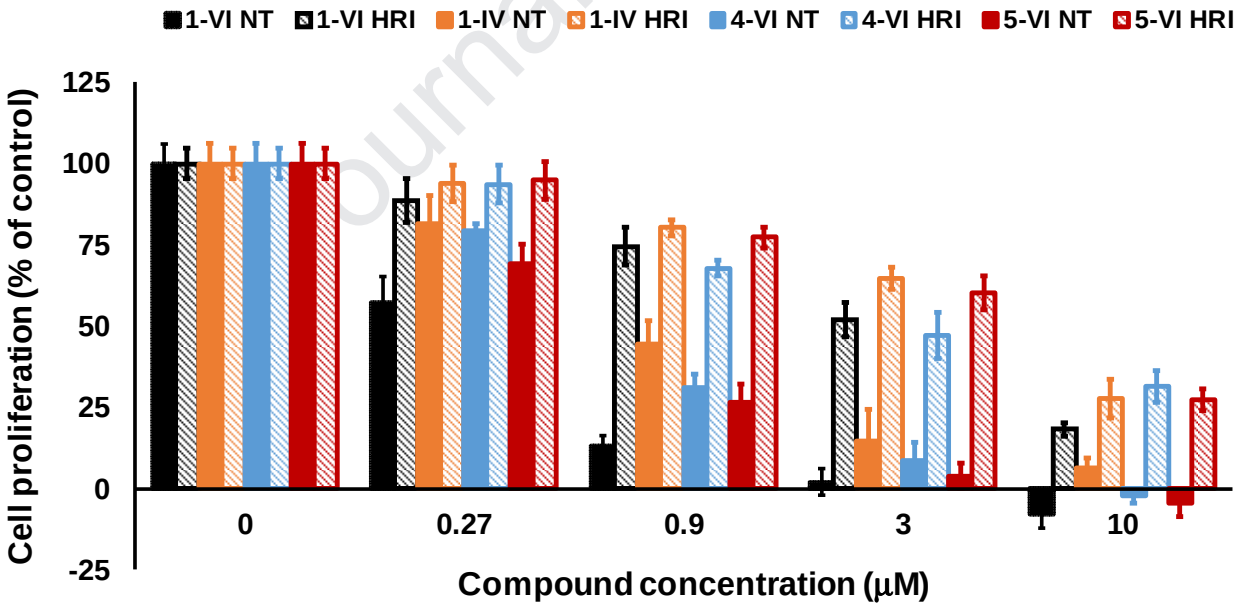

Figure 3. Inhibition of cell proliferation by lead compounds is dependent on HRI. MCF-7 cells transfected with (solid bars) or without (hatched bars) siRNA targeting HRI were treated with the indicated concentrations of each compound for three days starting

one day after transfection and cell proliferation was measured by sulforhodamine B assay as previously reported [9] (Also uploaded as a TIFF file)

Conclusions

The study reported herein is a continuation of our previously published studies that established the 1-phenyl-3-((1,4-*trans*)-4-phenoxycyclohexyl)ureas (ΦO*c*HΦUs) as a promising scaffold for activation of HRI and as such activators of eIF2α phosphorylation and subsequent inhibitors of translation initiation. The major objective of this study was to further optimize the leads **1-VI** and **2-VI**, identified previously, by lowering their lipophilicity and if possible enhance their potency. Removal of the CF_3 substituent from the *N*-phenyl in **1-VI** and replacing it with a F generating *N*-(3-F,5-CN)phenyl and *N*-(3-F,4-CN)phenyl moieties as in **4-VI** and **5-VI**, respectively, that were almost as potent as the previous leads but had significantly lower lipophilicity as estimated from their cLogP, both 5.23 (cf. 6.20 for **1-VI**). However, reducing lipophilicity by replacing the (1,4-*trans*)-disubstituted cyclohexyl ring with smaller cycloalkyls such as cyclobutyl and cyclopentyl resulted in lower potency in the DLR assay and therefore did not generate any advantageous compounds. Interestingly, replacement of the (1,4-*trans*)-disubstituted cyclohexyl ring with a 2,5-disubstituted pyrimidine ring led to significantly lower cLogPs but reduced apparent solubility and abolished potency as measured in the surrogate eIF2α phosphorylation assay. The planarity and aromatic nature of the pyrimidine ring and the putative extended rigidification originating from the potential formation of an intramolecular hydrogen bond within the pyrimidin-2-yl-urea motif do not accommodate interactions with the solvent or productive interactions with the cognate macromolecular

targets of these ligands. Taken together, these results may underscore the unique role of the (1,4-*trans*)-disubstituted cyclohexyl moiety as an advantageous linker connecting the two pharmacophore fragments, the *N*-phenyl-ureido and the phenoxy motif, allowing them acquire the correct spatial orientation and providing the right molecular flexibility, bulk and lipophilicity. Figure 4 depicts a potential mechanism of HRI activation by 4-CF_3-ΦO*c*HΦUs.

In addition, this study contributes two 4-CF_3-ΦO*c*HΦUs, **4-VI** and **5-VI**, as promising leads to the previously reported **1-VI** and **2-VI** and provides us with the molecular tools to explore their pharmacokinetic and pharmacodynamic properties in animals and as drug candidates in animal model of diseases such as cancer, neurodegenerative disorders and β-thalassemia. Finally, when employed in combination with other eIF2α kinase activators, these compounds are invaluable tools for dissecting contribution of eIF2α vs other substrates specific to each eIF2α kinase to normal- and patho-biology of those kinases.

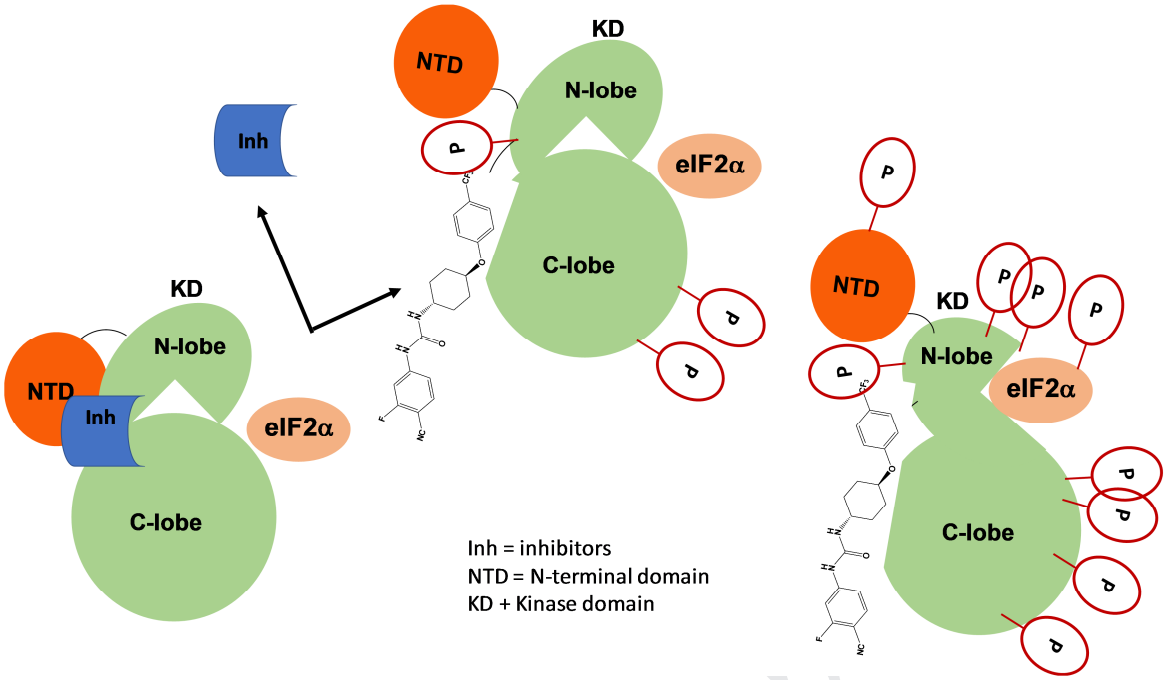

Figure 4. A hypothetical model of HRI activation by 4-CF_3-ΦO*c*HΦUs. HRI binding of heme or cellular chaperones such as HSP-90 and/or other endogenous inhibitors cause the N-terminal domain (NTD) to interact with kinase domain such that kinase domain is inactive cannot bind the eIF2α. The 4-CF_3-ΦO*c*HΦUs displace such inhibitors releasing the NTD from kinase domain which results a series of auto-phosphorylation events that changes the relative orientation of N-lobe and C-lobe of kinase domain rendering the substrate binding domain accessible to eIF2α binding and catalysis (also submitted separately in TIFF format)

4. Experimental

4.1. Materials and methods

4.1.1. General methods

All reagents and solvents were purchased from commercial sources and used as is. Analytical HPLC was run on a Waters Alliance 2695 using a reverse-phase column (XBridge BEH130 C18, 4.6 × 100 mm, particle size 5 μm) eluting with a linear gradient of acetonitrile in water containing 0.1% trifluoracetic acid (TFA). The purity of all target compounds was greater than 95% by analytical HPLC inspection. LC-MS analysis was run on a Waters Alliance 2695 with UV detector (214 and 254 nm) and Micromass ZQ

quadrupole mass detector in electrospray positive (ESI^+) mode using a reverse-phase column (Waters Symmetry C18, 2.1 × 100 mm, particle size 3.5 μm) eluting with a linear gradient of acetonitrile in water containing 0.1% formic acid. TLC analysis was run on Merck silica gel 60 F_{254} aluminum sheets. Flash chromatography purifications were performed on Biotage SP1 using silica gel prepacked normal phase columns (200−400 mesh) eluting with a linear gradient of ethyl acetate in n-heptane, and fractions were collected at 254 nm and monitored at 280 nm. Melting points were determined on a Mel-Temp electrothermal apparatus equipped with a Barnaand thermometer and were uncorrected. Proton, carbon, and fluorine NMR experiments were performed on a Varian Inova 400 MHz spectrometer using DMSO-d_6 as solvent. Chemical shifts (δ) are reported in ppm relative to TMS as the internal standard.

4.2. Chemistry

The synthesis, purification and characterization of **1-VI**, **2-VI** and **3-VI** were previously reported by us [11,12] and they are brought here for reference only.

*4.2.1. tert-Butyl (1S,3S)-3-(4-(trifluoromethyl)phenoxy)cyclopentylcarbamate (***A-V***)*

To a solution of *tert*-butyl (*1S,3R*)-3-hydroxycyclopentylcarbamate (0.50 g, 2.5 mmol) ,4-(trifluoromethyl)phenol (0.49 g, 3 mmol) and triphenylphosphine (0.98 g, 3.75 mmol) in anhydrous THF (8 mL) was dropwise added DIAD (0.98 mL, 4.68 mmol) in anhydrous THF (7 mL). The reaction solution was stirred at room temperature overnight. The resulting solution was concentrated *in vacuo*, and the residue was subjected to flash column chromatography on silica gel (eluting with EtOAc-heptane by a gradient of EtOAc from 4% to 32%) to deliver title compound as colorless crystals (0.63g, 73%); mp 129.3-132.1 ºC. ^{1}H NMR (400 MHz, DMSO-d_6) δ 7.60 (d, *J* = 8.7 Hz, 2H), 7.04 (d, *J* = 8.7 Hz, 2H), 6.93 (d, *J* = 6.8 Hz, 1H), 4.96 – 4.86 (m, 1H), 3.95 (dq, *J* = 13.8, 7.0 Hz, 1H), 2.15 (ddd, *J* = 20.2, 8.8, 6.2 Hz, 1H), 1.94 (td, *J* = 13.9, 7.3 Hz, 2H), 1.86 – 1.76 (m, 1H), 1.64 (ddd, *J* = 10.2, 8.6, 2.4 Hz, 1H), 1.52 – 1.39 (m, 1H), 1.36 (s, 9H). ^{13}C NMR (100

MHz, DMSO-d_6) δ 160.78 (d, *J* = 1.1 Hz), 155.51, 127.34 (q, *J* = 3.7 Hz), 125.03 (q, *J* = 270.8 Hz), 121.24 (q, *J* = 32.1 Hz), 116.10, 78.16, 50.48, 30.85, 30.64, 28.70. ^{19}F NMR (376 MHz, DMSO-d_6) δ -59.83.

*4.2.2. tert-Butyl trans-3-(4-(trifluoromethyl)phenoxy)cyclobutylcarbamate (***A-IV***)*

A-IV was prepared in essentially the same way as **A-V**. White solid (0.78 g, 94%); mp 137.8-141.8 ºC.^{1}H NMR (400 MHz, DMSO-d_6) δ 7.61 (d, *J* = 6.8 Hz, 2H), 7.28 (d, *J* = 5.0 Hz, 1H), 6.96 (d, *J* = 6.9 Hz, 2H), 4.86 (d, *J* = 2.7 Hz, 1H), 4.08 (d, *J* = 4.6 Hz, 1H), 2.41 – 2.22 (m, 4H), 1.36 (d, *J* = 2.4 Hz, 9H). ^{13}C NMR (100 MHz, DMSO-d_6) δ 160.50, 155.21, 127.42 (q, *J* = 3.7 Hz), 124.99 (q, *J* = 271.0 Hz), 121.57 (q, *J* = 32.2 Hz), 115.71, 70.04, 42.05, 36.89, 28.66. ^{19}F NMR (376 MHz, DMSO-d_6) δ -59.03.

*4.2.3. tert-Butyl cis-3-(4-(trifluoromethyl)phenoxy)cyclobutylcarbamate (***A-IVc***)*

A-IVc was prepared in essentially the same way as **A-V**. White solid (0.45 g, 27%); mp 157.0-159.0 ºC (CH_2Cl_2).^{1}H NMR (400 MHz, DMSO-d_6) δ 7.60 (d, *J* = 7.6 Hz, 2H), 7.18 (d, *J* = 7.2 Hz, 1H), 7.00 (d, *J* = 7.8 Hz, 2H), 4.52 – 4.30 (m, 1H), 3.69 (dd, *J* = 15.7, 8.0 Hz, 1H), 2.76 (d, *J* = 6.3 Hz, 2H), 1.97 (d, *J* = 8.2 Hz, 2H), 1.36 (s, 9H). ^{13}C NMR (100 MHz, DMSO-d_6) δ 160.38 (d, *J* = 1.3 Hz), 155.02, 127.42 (q, *J* = 3.7 Hz), 124.98 (q, *J* = 270.6 Hz), 121.59 (q, *J* = 32.1 Hz), 115.64, 65.68, 38.51, 37.65, 28.66. ^{19}F NMR (376 MHz, DMSO-d_6) δ -59.11.

4.2.4. (1S,3S)-3-(4-(Trifluoromethyl)phenoxy)cyclopentanamine (**B-V**)

A-V (518 mg, 1.5 mmol) was dissolved in anhydrous methylene chloride (10 mL), and a solution of trifluoroacetic acid (5.31 g, 45 mmol) in anhydrous methylene chloride (5 mL) was added. The reaction solution was stirred at room temperature for 1h. The resulting solution was rotavapored, and the residue was diluted in methylene chloride (60 mL), washed with saturated aqueous sodium bicarbonate (2×20 mL), dried over anhydrous sodium sulfate, and evaporated *in vacuo* to deliver title compound as semi-solid (380 mg, 103%) that was used in the next step without further purification. ^{1}H NMR (400 MHz, DMSO-d_6) δ 7.59 (d, *J* = 8.7 Hz, 2H), 7.02 (d, *J* = 8.6 Hz, 2H), 4.93 (m, 2H), 3.41 (m, 1H), 2.22 (m, 1H), 2.01 – 1.81 (m, 2H), 1.76 – 1.66 (m, 1H), 1.66 – 1.55 (m, 1H), 1.29 (m, 1H), 1.39 – 1.17 (m, 1H). ^{19}F NMR (376 MHz, DMSO-d_6) δ -59.77.

4.2.5. trans-3-(4-(Trifluoromethyl)phenoxy)cyclobutanamine (**B-IV**)

B-IV was prepared in essentially the same way as **B-V**. Yellow semi-solid (0.49 g, 100%). ^{1}H NMR (400 MHz, DMSO-d_6) δ 7.60 (d, *J* = 8.7 Hz, 2H), 6.95 (d, *J* = 8.6 Hz, 2H), 4.99 – 4.77 (m, 2H), 3.70 – 3.45 (m, 1H), 2.25 (ddd, *J* = 11.9, 7.5, 4.1 Hz, 2H), 2.14 (dt, *J* = 12.3, 6.1 Hz, 2H). ^{13}C NMR (100 MHz, DMSO-d_6) δ 160.70, 127.39 (q, *J* = 3.8 Hz), 125.02 (q, *J* = 271.0 Hz), 121.37 (q, *J* = 31.7 Hz), 115.70, 70.57, 43.93, 39.61. ^{19}F NMR (376 MHz, DMSO-d_6) δ -59.84.

4.2.6. cis-3-(4-(Trifluoromethyl)phenoxy)cyclobutan-1-amine (**B-IVc**)

B-IVc was prepared in essentially the same way as **B-V**. Off white solid (0.28 g, 100%); mp 71.9-74.3 ºC.

4.2.7. 5-(4-(Trifluoromethyl)phenoxy)pyrimidin-2-amine (**B-py**)

A mixture of 2-aminopyrimidin-5-ol (0.5 g, 4.5 mmol), 1-fluoro-4-(trifluoromethyl)benzene (0.74 g, 4.5 mmol) and cesium carbonate (4.4 g, 13.5 mmol) in DMSO (8 mL) were stirred under argon at 80 ºC for 5h. The resulting reaction was diluted with ethyl acetate (90 mL) and water (30 mL). Aqueous phase was back-extracted with ethyl acetate (60 mL). Combined extract was washed with brine (5×30 mL), dried over anhydrous sodium sulfate overnight, and evaporated in vacuo. The residue was recrystallized from hot ethyl acetate to deliver title compound as white crystalline solid (0.12 g, 10%); mp 132.5-134.5 ºC (EtOAc). ^{1}H NMR (400 MHz, DMSO-d_6) δ 8.20 (s, 2H), 7.68 (d, *J* = 8.7 Hz, 2H), 7.10 (d, *J* = 8.6 Hz, 2H), 6.73 (s, 2H). ^{13}C NMR (100 MHz, DMSO-d_6) δ 161.95 (d, *J* = 1.3 Hz), 161.85, 151.94, 141.27, 127.85 (q, *J* = 3.8 Hz), 124.73 (q, *J* = 271.2 Hz), 123.38 (q, *J* = 32.2 Hz), 116.78. ^{19}F NMR (376 MHz, DMSO-d_6) δ -60.15.

4.2.8. 1-(3-Cyano-5-fluorophenyl)-3-(trans-4-(4-(trifluoromethyl)phenoxy)cyclohexyl)urea (**4-VI**)

3-Amino-5-fluorobenzonitrile (0.41 g, 3 mmol) and anhydrous pyridine (0.36 g, 4.5 mmol) were dissolved in anhydrous methylene chloride (45 mL). Phenyl chloroformate (0.70 g, 4.5 mmol) was added dropwise at 0 ºC. The reaction was stirred under argon at room temperature for 4 h. The resulting solution was washed with consecutively with 1 mol/L aqueous hydrochloride, water and brine, dried over anhydrous sodium sulfate, and evaporated *in vacuo* to deliver phenyl (3-cyano-5-fluorophenyl)carbamate (**E-4**) as white solid in quantitative yield and used as it without further purification.

Above obtained **E-4** (0.13 g, 0.5 mmol) and

trans-4-(4-(trifluoromethyl)phenoxy)cyclohexan-1-amine (**B-VI**) (0.13 g, 0.5 mmol) in anhydrous pyridine (9 mL) were stirred under argon at 80 ºC for 4 h. The resulting reaction solution was evaporated *in vacuo*, and the residue was crystallized from hot ethyl acetate to deliver the title compound as crystalline white solid (105 mg, 50%); mp 237.8-240.8 ºC (EtOAc). ^{1}H NMR (400 MHz, DMSO-d_6) δ 8.84 (s, 1H), 7.64 (dt, *J* = 11.8, 2.2 Hz, 1H), 7.59 (d, *J* = 8.8 Hz, 2H), 7.58 – 7.57 (m, 1H), 7.28 (ddd, *J* = 8.3, 2.3, 1.3 Hz, 1H), 7.11 (d, *J* = 8.7 Hz, 2H), 6.47 (d, *J* = 7.6 Hz, 1H), 4.52 – 4.36 (m, 1H), 3.59 – 3.47 (m, 1H), 2.16 – 1.95 (m, 2H), 1.95 – 1.79 (m, 2H), 1.58 – 1.27 (m, 4H). ^{13}C NMR (100 MHz, DMSO-d_6) δ 162.42 (d, *J* = 243.3 Hz), 160.72 (d, *J* = 1.1 Hz), 154.45, 143.82 (d, *J* = 12.1 Hz), 127.36 (q, *J* = 3.9 Hz), 125.01 (d, *J* = 271.0 Hz), 121.27 (d, *J* = 32.0 Hz), 118.30 (d, *J* = 3.8 Hz), 117.29 (d, *J* = 2.7 Hz), 116.26, 113.06 (d, *J* = 12.3 Hz), 111.39 (d, *J* = 25.6 Hz), 109.46 (d, *J* = 26.3 Hz), 74.83, 47.74, 30.19, 29.94. ^{19}F NMR (376 MHz, DMSO-d_6) δ -59.82, -109.68 (dd, *J* = 11.7, 8.4 Hz). LC-MS (ESI): *m/z* 422.09$[M+H]^+$, 463.10 $[M+H+41]^+$.

4.2.9.
1-(5-Fluoro-2-methylphenyl)-3-((1S,3S)-3-(4-(trifluoromethyl)phenoxy)cyclopentyl)urea (**7-V**)

B-V (61 mg, 0.25 mmol) was dissolved in anhydrous ethyl acetate (4 mL), and a solution of 4-fluoro-2-isocyanato-1-methylbenzene (40 mg, 0.26 mmol) in anhydrous ethyl acetate (3.5 mL) was added dropwise at 55-60 ºC. The reaction solution was stirred at 60 ºC for 2h, and evaporated *in vacuo*. The resulting solid residue was recrystallized from hot ethyl acetate to deliver the title compound **7-V** as white crystalline solid (58 mg, 59%); mp 209.8-211.4 ºC (EtOAc). ^{1}H NMR (400 MHz, DMSO-d_6) δ 7.84 (dd, *J* = 12.5, 2.7 Hz, 1H), 7.63 (d, *J* = 2.6 Hz, 1H), 7.61 (d, *J* = 8.8 Hz, 2H), 7.11 – 7.07 (m, 1H), 7.06 (d, *J* = 8.6 Hz, 2H), 6.87 (d, *J* = 6.9 Hz, 1H), 6.62 (td, *J* = 8.3, 2.8 Hz, 1H), 5.03 – 4.91 (m, 1H), 4.24 – 4.06 (m, 1H), 2.22 (ddd, *J* = 20.3, 8.9, 6.2 Hz, 1H), 2.12 (s, 3H), 2.10 – 2.01 (m, 2H), 1.88 – 1.78 (m, 1H), 1.78 – 1.67 (m, 1H), 1.47 (dt, *J* = 16.0, 7.1 Hz, 1H). ^{13}C NMR (100 MHz, DMSO-d_6) δ 161.07 (d, *J* = 237.5 Hz), 160.75 (d, *J* = 1.1 Hz), 155.09, 140.11 (d, *J* = 11.7 Hz), 131.31 (d, *J* = 9.5 Hz), 127.36 (q, *J* = 3.8 Hz), 125.03 (q, *J* = 271.0 Hz), 121.31 (q, *J* = 32.0 Hz), 121.30 (d, *J* = 2.9 Hz), 116.14, 107.66 (d, *J* = 21.1 Hz), 105.94 (d, *J* = 27.3 Hz), 78.11, 49.86, 31.28, 30.82, 17.59. ^{19}F NMR (376 MHz, DMSO-d_6) δ -59.83, -116.01 (m). LC-MS (ESI): *m/z* 397.35 $[M+H]^+$, 438.42 $[M+H+41]^+$.

4.2.10. Cyclobutyl series (**IV**)

4.2.10.1.1-(3-Cyano-5-(trifluoromethyl)phenyl)-3-(trans-3-(4-(trifluoromethyl)phenoxy)cyclobutyl)urea (**1-IV**)

Prepared in essentially the same way as **4-VI**. White solid (60 mg, 27%); mp 191.6-193.0 ºC (EtOAc). ^{1}H NMR (400 MHz, DMSO-d_6) δ 9.09 (s, 1H), 8.15 (s, 1H), 8.03 (s, 1H), 7.77 (s, 1H), 7.62 (d, *J* = 8.7 Hz, 2H), 7.02 (d, *J* = 7.0 Hz, 1H), 6.99 (d, *J* = 8.7 Hz, 2H), 4.99 – 4.85 (m, 1H), 4.40 – 4.21 (m, 1H), 2.55 – 2.35 (m, 4H). ^{13}C NMR (100 MHz, DMSO-d_6) δ 160.49 (d, *J* = 1.2 Hz), 154.62, 142.67, 131.13 (q, *J* = 32.0 Hz), 127.45 (d, *J* = 3.7 Hz), 125.00 (q, *J* = 270.0 Hz), 124.58, 123.57 (q, *J* = 272.0 Hz), 121.63 (q, *J* = 32.0 Hz), 121.30 (m), 118.60 (m), 118.06, 115.76, 113.27, 70.13, 41.91, 36.93. ^{19}F NMR (376 MHz, DMSO-d_6) δ -59.88, -61.91. LC-MS (ESI): *m/z* 444.05 $[M+H]^+$, 485.12 $[M+H+41]^+$.

4.2.10.2.
1-(trans-3-(4-(Trifluoromethyl)phenoxy)cyclobutyl)-3-(3-(trifluoromethyl)phenyl)urea (**2-IV**)

Prepared in essentially the same way as **7-V**. White solid (45 mg, 22%); mp 171.8-174.6 ºC (EtOAc). ^{1}H NMR (400 MHz, DMSO-d_6) δ 8.78 (s, 1H), 7.94 (s, 1H), 7.63 (d, *J* = 8.6 Hz, 2H), 7.51 (d, *J* = 8.5 Hz, 1H), 7.43 (t, *J* = 7.9 Hz, 1H), 7.21 (d, *J* = 7.6 Hz, 1H), 7.00 (d, *J* = 8.6 Hz, 2H), 6.74 (d, *J* = 7.0 Hz, 1H), 4.97 – 4.86 (m, 1H), 4.40 – 4.19 (m, 1H), 2.49 – 2.28 (m, 4H). ^{13}C NMR (100 MHz, DMSO-d_6) δ 160.52 (d, *J* = 1.1 Hz), 154.93, 141.63, 130.14, 129.83 (q, *J* = 31.2 Hz), 127.46 (q, *J* = 3.7 Hz), 125.00 (q, *J* = 270.0 Hz), 121.79 (d, *J* = 1.0 Hz), 121.60 (q, *J* = 32.2 Hz), 117.80 (q, *J* = 3.8 Hz), 115.78, 114.17 (q, *J* = 4.0 Hz), 70.17, 41.81, 37.08. ^{19}F NMR (376 MHz, DMSO-d_6) δ -59.85, -61.35. LC-MS (ESI): *m/z* 419.11 $[M+H]^+$, 460.19 $[M+H+41]^+$.

4.2.10.3. 1-(3-Cyanophenyl)-3-(trans-3-(4-(trifluoromethyl)phenoxy)cyclobutyl)urea (**3-IV**)

Prepared in essentially the same way as **7-V**. Off white solid (75 mg, 40%); mp 181.1-182.3 ºC (EtOAc). ^{1}H NMR (400 MHz, DMSO-d_6) δ 8.77 (s, 1H), 7.90 (s, 1H), 7.63 (d, *J* = 8.7 Hz, 1H), 7.59 (dd, *J* = 8.5, 0.9 Hz, 1H), 7.41 (t, *J* = 7.9 Hz, 1H), 7.32 (d, *J* = 7.6 Hz, 1H), 7.00 (d, *J* = 8.7 Hz, 2H), 6.80 (d, *J* = 7.0 Hz, 1H), 4.99 – 4.84 (m, 1H), 4.29 (m, 1H), 2.48 – 2.27 (m, 4H). ^{13}C NMR (100 MHz, DMSO-d_6) δ 160.51 (d, *J* = 1.1 Hz), 154.82, 141.68, 130.46, 127.46 (q, *J* = 3.8 Hz), 125.06, 125.00 (q, *J* = 270.0 Hz), 122.86, 121.61 (q, *J* = 32.0 Hz), 120.75, 119.39, 115.78, 111.87, 70.16, 41.80, 37.07. ^{19}F NMR (376 MHz, DMSO-d_6) δ -59.84. LC-MS (ESI): *m/z* 376.18 $[M+H]^+$, 417.19 $[M+H+41]^+$.

4.2.10.4.
1-(3-Cyano-5-fluorophenyl)-3-(trans-3-(4-(trifluoromethyl)phenoxy)cyclobutyl)urea

(**4-IV**)

Prepared in essentially the same way as **4-VI**. White crystals (110 mg, 56%); mp 182.8-185.0 ºC (EtOAc). ^{1}H NMR (400 MHz, DMSO-d_6) δ 8.96 (s, 1H), 7.65 (d, *J* = 13.3 Hz, 1H), 7.62 (d, *J* = 8.9 Hz, 2H), 7.29 (d, *J* = 7.5 Hz, 1H), 6.99 (d, *J* = 8.5 Hz, 2H), 6.94 (d, *J* = 6.9 Hz, 1H), 4.96 – 4.86 (m, 1H), 4.34 – 4.23 (m, 1H), 2.42 (ddd, *J* = 16.3, 12.5, 5.0 Hz, 6H). ^{13}C NMR (100 MHz, DMSO-d_6) δ 162.38 (d, *J* = 243.6 Hz), 160.49 (d, *J* = 0.9 Hz), 154.55, 143.73 (d, *J* = 12.1 Hz), 127.44 (q, *J* = 3.7 Hz), 124.99 (q, *J* = 271.0 Hz), 121.63 (q, *J* = 32.1 Hz), 118.28 (d, *J* = 4.0 Hz), 117.55 (d, *J* = 2.7 Hz), 115.76, 113.03 (d, *J* = 12.3 Hz), 111.57 (d, *J* = 25.6 Hz), 109.72 (d, *J* = 26.6 Hz), 70.13, 41.84, 36.98. ^{19}F NMR (376 MHz, DMSO-d_6) δ -59.87, -109.69 (dd, J = 11.6, 8.4 Hz). LC-MS (ESI): *m/z* 394.37 $[M+H]^+$, 435.32 $[M+H+41]^+$.

4.2.10.5.
1-(5-Fluoro-2-methylphenyl)-3-(trans-3-(4-(trifluoromethyl)phenoxy)cyclobutyl)urea
(**7-IV**)

Prepared in essentially the same way as **7-V**. White crystals (130 mg, 68%); mp 204.2-206.0 ºC (EtOAc). ^{1}H NMR (400 MHz, DMSO-d_6) δ 7.81 (dd, *J* = 12.4, 2.7 Hz, 1H), 7.70 (s, 1H), 7.63 (d, *J* = 8.6 Hz, 2H), 7.16 (d, *J* = 6.8 Hz, 1H), 7.13 – 7.07 (m, 1H), 7.00 (d, *J* = 8.6 Hz, 2H), 6.64 (td, *J* = 8.3, 2.8 Hz, 1H), 4.92 (p, *J* = 5.2 Hz, 1H), 4.35 – 4.22 (m, 1H), 2.46 – 2.38 (m, 4H), 2.14 (s, 3H). ^{13}C NMR (100 MHz, DMSO-d_6) δ 161.04 (d, *J* = 237.7 Hz), 160.50 (d, *J* = 1.0 Hz), 154.85 (s), 139.95 (d, *J* = 11.6 Hz), 131.36 (d, *J* = 9.4 Hz), 127.45 (q, *J* = 3.7 Hz), 125.00 (q, *J* = 271.1 Hz), 121.63 (d, *J* = 32.2 Hz), 121.62 (m), 115.79, 107.90 (d, *J* = 21.2 Hz), 106.21 (d, *J* = 27.4 Hz), 70.20, 41.66, 37.20, 17.58. ^{19}F NMR (376 MHz, DMSO-d_6) δ -59.86, -116.04 (m). LC-MS (ESI): *m/z* 383.32 $[M+H]^+$, 424.40 $[M+H+41]^+$.

4.2.10.6. 1-(3,4-difluorophenyl)-3-(trans-3-(4-(trifluoromethyl)phenoxy)cyclobutyl)urea
(**10-IV**)

Prepared in essentially the same way as **7-V**. White solid (63 mg, 33%); mp 179.9-182.0 ºC. ^{1}H NMR (400 MHz, DMSO-d_6) δ 8.62 (s, 1H), 7.62 (d, *J* = 8.6 Hz, 2H), 7.61 – 7.55 (m, 1H), 7.25 (dd, *J* = 19.7, 9.3 Hz, 1H), 7.05 – 7.01 (m, 1H), 6.99 (d, *J* = 8.6 Hz, 2H), 6.68 (d, *J* = 7.0 Hz, 1H), 4.97 – 4.84 (m, 1H), 4.37 – 4.19 (m, 1H), 2.41 (m, 4H). ^{13}C NMR (100 MHz, DMSO-d_6) δ 160.52 (d, *J* = 1.3 Hz), 154.89, 149.47 (dd, *J* = 242.0, 13.3 Hz), 144.45 (dd, *J* = 238.6, 12.7 Hz), 137.97 (dd, *J* = 9.5, 2.5 Hz), 127.45 (q, *J* = 3.8 Hz), 125.00 (q, *J* = 271.0 Hz), 121.60 (q, *J* = 32.1 Hz), 117.59 (d, *J* = 18.6 Hz), 115.77, 114.23 (dd, *J* = 5.7, 3.2 Hz), 107.07 (d, *J* = 21.8 Hz), 70.16, 41.78, 37.11. ^{19}F NMR (376 MHz, DMSO-d_6) δ -59.86, -137.83 (ddd, J = 23.1, 13.5, 9.4 Hz), -148.15 (m). LC-MS (ESI): *m/z*

387.22 $[M+H]^+$, 428.24 $[M+H+41]^+$.

4.2.10.7. 1-(2,3-difluorophenyl)-3-(trans-3-(4-(trifluoromethyl)phenoxy)cyclobutyl)urea (**11-IV**)

Prepared in essentially the same way as **7-V**. White crystals (120 mg, 69%); mp 205.9-208.0 ºC (EtOAc-heptane). ^{1}H NMR (400 MHz, DMSO-d_6) δ 8.83 (s, 1H), 7.62 (d, *J* = 8.6 Hz, 2H), 7.11 (m, 1H), 6.99 (d, *J* = 8.6 Hz, 2H), 6.80 (d, *J* = 6.9 Hz, 1H), 6.73 – 6.59 (m, 1H), 5.00 – 4.82 (m, 1H), 4.42 – 4.11 (m, 1H), 2.41 (m, 4H). ^{13}C NMR (100 MHz, DMSO-d_6) δ 163.08 (d, *J* = 241.8 Hz), 162.92 (d, *J* = 241.8 Hz), 160.50, 154.61, 143.47 (d, *J* = 13.8 Hz), 127.44 (q, *J* = 3.7 Hz), 124.99 (d, *J* = 270.9 Hz), 121.61 (d, *J* = 32.1 Hz), 115.76, 101.01, 100.71, 96.30 (d, *J* = 27.4 Hz), 70.14, 41.77, 37.03. ^{19}F NMR (376 MHz, DMSO-d_6) δ -59.87, -110.04 (d, *J* = 9.4 Hz), -110.06 (d, *J* = 9.4 Hz). LC-MS (ESI): *m/z* 387.29 $[M+H]^+$, 428.37 $[M+H+41]^+$.

4.2.10.8. 1-(3-Cyano-5-(trifluoromethyl)phenyl)-3-(cis-3-(4-(trifluoromethyl)phenoxy)cyclobutyl)urea (**1-IV*c***)

Prepared in essentially the same way as **4-VI**. White solid (80 mg, 62%); mp 194.6-196.1 ºC (EtOAc). ^{1}H NMR (400 MHz, DMSO-d_6) δ 9.08 (s, 1H), 8.13 (s, 1H), 8.03 (s, 1H), 7.77 (s, 1H), 7.62 (d, *J* = 8.6 Hz, 2H), 7.03 (d, *J* = 8.6 Hz, 2H), 6.94 (d, *J* = 7.8 Hz, 1H), 4.54 (p, *J* = 6.9 Hz, 1H), 4.02–3.81 (m, 1H), 2.87 (m, 2H), 2.05 (td, J = 9.1, 2.8 Hz, 2H). ^{13}C NMR (100 MHz, DMSO-d_6) δ 160.34 (d, *J* = 1.2 Hz), 154.37, 142.67, 131.11 (q, *J* = 33.0 Hz), 127.46 (q, *J* = 3.7 Hz), 124.97 (q, *J* = 270.9 Hz), 124.60, 123.57 (q, *J* = 272.7 Hz), 121.66 (q, *J* = 32.0 Hz), 121.30 (q, *J* = 3.7 Hz), 118.63 (q, *J* = 3.9 Hz), 118.06, 115.67, 113.26, 65.86, 38.69, 37.32. ^{19}F NMR (376 MHz, DMSO-d_6) δ -59.88, -61.89. LC-MS (ESI): *m/z* 444.05 $[M+H]^+$, 485.12 $[M+H+41]^+$.

4.2.10.9. 1-(cis-3-(4-(Trifluoromethyl)phenoxy)cyclobutyl)-3-(3-(trifluoromethyl)phenyl)urea (**2-IV*c***)

Prepared in essentially the same way as **7-V**. White solid (40 mg, 32%); mp 166.6-168.5 ºC. ^{1}H NMR (400 MHz, DMSO-d_6) δ 8.84 (s, 1H), 8.01 (s, 1H), 7.70 (d, *J* = 8.7 Hz, 2H), 7.58 (d, *J* = 8.5 Hz, 1H), 7.50 (t, *J* = 7.9 Hz, 1H), 7.29 (d, *J* = 7.6 Hz, 1H), 7.12 (d, *J* = 8.6 Hz, 2H), 6.73 (d, *J* = 7.9 Hz, 1H), 4.62 (p, *J* = 7.1 Hz, 1H), 4.09 – 3.91 (m, 1H), 3.06 – 2.85 (m, 2H), 2.20 – 2.01 (m, 2H). ^{13}C NMR (100 MHz, DMSO-d_6) δ 160.37 (d, *J* = 1.1 Hz), 154.66, 141.62, 130.14, 129.81 (d, *J* = 31.2 Hz), 127.46 (q, *J* = 3.7 Hz), 124.98 (d, *J*

= 270.9 Hz), 124.70 (d, *J* = 272.3 Hz), 121.81 (d, *J* = 1.2 Hz), 121.64 (d, *J* = 32.5 Hz), 117.81 (q, *J* = 7.6, 4.0 Hz), 115.69, 114.19 (q, *J* = 7.9, 4.1 Hz), 65.87, 38.88, 37.22. ^{19}F NMR (376 MHz, DMSO-d_6) δ -59.86, -61.35. LC-MS (ESI): *m/z* 418.98 $[M+H]^+$, 460.05 $[M+H+41]^+$.

4.2.10.10. 1-(3-Cyanophenyl)-3-(cis-3-(4-(trifluoromethyl)phenoxy)cyclobutyl)urea (**3-IV*c***)

Prepared in essentially the same way as **7-VI**. Off white solid (180 mg, 96%); mp 203.7-206.8 ºC. ^{1}H NMR (400 MHz, DMSO-d_6) δ 8.74 (s, 1H), 7.90 (t, *J* = 1.7 Hz, 1H), 7.62 (d, *J* = 8.7 Hz, 2H), 7.60 – 7.56 (m, 1H), 7.40 (t, *J* = 7.9 Hz, 1H), 7.31 (m, 1H), 7.03 (d, *J* = 8.6 Hz, 2H), 6.70 (d, *J* = 7.9 Hz, 1H), 4.53 (p, *J* = 7.0 Hz, 1H), 4.02 – 3.83 (m, 1H), 2.97 – 2.77 (m, 2H), 2.01 (m, 2H). ^{13}C NMR (100 MHz, DMSO-d_6) δ 160.36 (d, *J* = 1.1 Hz), 154.56, 141.68, 130.44, 127.45 (q, *J* = 3.7 Hz), 125.06, 124.98 (q, *J* = 271.0 Hz), 122.88, 121.65 (q, *J* = 32.0 Hz), 120.78, 119.39, 115.67, 111.87, 65.86, 38.87, 37.21. ^{19}F NMR (376 MHz, DMSO-d_6) δ -59.87. LC-MS (ESI): *m/z* 376.11 $[M+H]^+$, 417.12 $[M+H+41]^+$.

4.2.11. Cyclopentyl series (**V**)

4.2.11.1. 1-(3-Cyano-5-(trifluoromethyl)phenyl)-3-((1S,3S)-3-(4-(trifluoromethyl)phenoxy)cyclopentyl)urea (**1-V**)

Prepared in essentially the same way as **4-VI**. White solid (80 mg, 70%); mp 144.4-146.2 ºC (EtOAc-heptane). ^{1}H NMR (400 MHz, DMSO-d_6) δ 8.99 (s, 1H), 8.14 (s, 1H), 8.00 (s, 1H), 7.76 (s, 1H), 7.61 (d, *J* = 8.7 Hz, 2H), 7.06 (d, *J* = 8.6 Hz, 2H), 6.69 (d, *J* = 7.2 Hz, 1H), 5.04 – 4.90 (m, 1H), 4.29 – 4.05 (m, 1H), 2.33 – 2.11 (m, 1H), 2.06 (dt, *J* = 13.3, 7.0 Hz, 2H), 1.96 – 1.80 (m, 1H), 1.80 – 1.62 (m, 1H), 1.51 (dt, *J* = 16.1, 7.3 Hz, 1H). ^{13}C NMR (100 MHz, DMSO-d_6) δ 160.73 (d, *J* = 1.1 Hz), 154.83, 142.73, 131.14 (q, *J* = 32.8 Hz), 127.37 (d, *J* = 3.8 Hz), 125.02 (d, *J* = 270.8 Hz), 124.43, 123.58 (q, *J* = 272.9 Hz), 121.63 (q, *J* = 31.9 Hz), 121.17 (q, *J* = 2.7 Hz), 118.44 (q, *J* = 3.9 Hz), 118.06, 116.13, 113.28, 78.11, 50.01, 31.01, 30.78. ^{19}F NMR (376 MHz, DMSO-d_6) δ -59.83, -61.91. LC-MS (ESI): *m/z* 458.33 $[M+H]^+$, 499.34 $[M+H+41]^+$.

4.2.11.2. 1-((1S,3S)-3-(4-(Trifluoromethyl)phenoxy)cyclopentyl)-3-(3-(trifluoromethyl)phenyl)urea (**2-V**)

Prepared in essentially the same way as **7-V**. Off white solid (60 mg, 56%); mp 123.5-125.3 ºC (EtOAc-heptane). ^{1}H NMR (400 MHz, DMSO-d_6) δ 8.68 (s, 1H), 7.95 (s, 1H), 7.61 (d, *J* = 8.7 Hz, 2H), 7.51–7.37 (m, 2H), 7.19 (d, *J* = 7.4 Hz, 1H), 7.06 (d, *J* = 8.7 Hz, 2H), 6.40 (d, *J* = 7.2 Hz, 1H), 5.02 – 4.90 (m, 1H), 4.25–4.07 (m, 1H), 2.21 (ddd, *J* = 20.3, 9.0, 6.1 Hz, 1H), 2.14–1.98 (m, 2H), 1.92–1.79 (m, 1H), 1.79–1.63 (m, 1H), 1.49 (m, 1H). ^{13}C NMR (100 MHz, DMSO-d_6) δ 160.75 (d, *J* = 1.4 Hz), 155.15, 141.71, 130.13, 129.85 (q, *J* = 31.3 Hz), 127.37 (q, *J* = 3.8 Hz), 125.03 (d, *J* = 270.7 Hz), 124.70 (q, *J* = 272.2 Hz),121.61, 121.30 (q, *J* = 32.1 Hz), 117.66 (q, *J* = 3.7 Hz), 116.13, 113.99 (q, *J* = 4.1 Hz), 78.13, 49.90, 31.15, 30.79. ^{19}F NMR (376 MHz, DMSO-d_6) δ -59.82, -61.38. LC-MS (ESI): *m/z* 433.13 $[M+H]^+$, 474.21 $[M+H+41]^+$.

4.2.11.3. 1-(3-Cyanophenyl)-3-((1S,3S)-3-(4-(trifluoromethyl)phenoxy)cyclopentyl)urea (**3-V**)

Prepared in essentially the same way as **7-V**. White solid (65 mg, 67%); mp 160.2-162.1 ºC (EtOAc-heptane). ^{1}H NMR (400 MHz, DMSO-d_6) δ 8.66 (s, 1H), 7.90 (t, *J* = 1.7 Hz, 1H), 7.61 (d, *J* = 8.7 Hz, 2H), 7.56 (dd, *J* = 8.3, 1.1 Hz, 1H), 7.40 (t, *J* = 7.9 Hz, 1H), 7.34 – 7.27 (m, 1H), 7.06 (d, *J* = 8.6 Hz, 2H), 6.46 (d, *J* = 7.2 Hz, 1H), 5.02 – 4.90 (m, 1H), 4.24 – 4.07 (m, 1H), 2.21 (ddd, *J* = 20.2, 9.0, 6.1 Hz, 1H), 2.06 (ddd, *J* = 20.4, 13.8, 7.0 Hz, 2H), 1.85 (ddd, *J* = 14.1, 7.9, 6.4 Hz, 1H), 1.79 – 1.63 (m, 1H), 1.55 – 1.40 (m, 1H). ^{13}C NMR (100 MHz, DMSO-d_6) δ 160.75 (d, *J* = 1.2 Hz), 155.04, 141.77, 130.45, 127.37 (q, *J* = 3.8 Hz), 125.03 (q, *J* = 270.9 Hz), 124.92, 122.68, 121.30 (q, *J* = 32.1 Hz), 120.57, 119.40, 116.13, 111.89, 78.12, 49.91, 31.15, 30.79. ^{19}F NMR (376 MHz, DMSO-d_6) δ -59.82. LC-MS (ESI): *m/z* 390.33 $[M+H]^+$, 431.35 $[M+H+41]^+$.

4.2.11.4. 1-(3-Cyano-5-fluorophenyl)-3-((1S,3S)-3-(4-(trifluoromethyl)phenoxy)cyclopentyl)urea (**4-V**)

Prepared in essentially the same way as **4-VI**. Off white solid (50 mg, 49%); mp 176.2-177.8 ºC (EtOAc-heptane). ^{1}H NMR (400 MHz, DMSO-d_6) δ 8.86 (s, 1H), 7.65 (s, 1H), 7.61 (d, *J* = 8.9 Hz, 2H), 7.61 (d, *J* = 13.9 Hz, 1H), 7.33 – 7.22 (m, 1H), 7.06 (d, *J* = 8.6 Hz, 2H), 6.61 (d, *J* = 7.2 Hz, 1H), 5.04 – 4.88 (m, 1H), 4.26 – 4.07 (m, 1H), 2.21 (m, 1H), 2.06 (m, 2H), 1.93 – 1.79 (m, 1H), 1.71 (m, 1H), 1.49 (m, 1H). ^{13}C NMR (100 MHz, DMSO-d_6) δ 162.40 (d, *J* = 243.3 Hz), 160.73 (d, *J* = 1.2 Hz), 154.77, 143.80 (d, *J* = 12.2 Hz), 127.37 (q, *J* = 3.8 Hz), 125.02 (d, *J* = 271.0 Hz), 121.31 (d, *J* = 32.1 Hz), 118.29 (d, *J* = 3.7 Hz), 117.40 (d, *J* = 2.6 Hz), 116.13, 113.04 (d, *J* = 12.3 Hz), 111.45 (d, *J* = 25.6 Hz), 109.57 (d, *J* = 26.2 Hz), 78.10, 49.95, 31.06, 30.78. ^{19}F NMR (376 MHz, DMSO-d_6) δ -59.82, -109.71 (dd, J = 11.7, 8.4 Hz). LC-MS (ESI): *m/z* 408.1 $[M+H]^+$, 449.1

$[M+H+41]^+$.

4.2.11.5.
1-(3,4-Difluorophenyl)-3-((1S,3S)-3-(4-(trifluoromethyl)phenoxy)cyclopentyl)urea (**10-V**)

Prepared in essentially the same way as **7-V**. White solid (40 mg, 34%); mp 175.4-177.5 ºC. ^{1}H NMR (400 MHz, DMSO-d_6) δ 8.52 (s, 1H), 7.61 (d, *J* = 8.9 Hz, 2H), 7.58 (dd, *J* = 7.6, 2.6 Hz, 1H), 7.24 (dd, *J* = 19.8, 9.2 Hz, 1H), 7.06 (d, *J* = 8.6 Hz, 2H), 7.02 – 6.96 (m, 1H), 6.34 (d, *J* = 7.2 Hz, 1H), 5.01 – 4.89 (m, 1H), 4.23 – 4.06 (m, 1H), 2.20 (ddd, *J* = 20.3, 8.9, 6.0 Hz, 1H), 2.05 (ddd, *J* = 20.1, 13.6, 6.8 Hz, 2H), 1.90 – 1.77 (m, 1H), 1.77 – 1.62 (m, 1H), 1.47 (dt, *J* = 16.1, 7.3 Hz, 1H). ^{13}C NMR (100 MHz, DMSO-d_6) δ 160.74, 155.12, 149.49 (dd, *J* = 241.8, 13.0 Hz), 144.36 (dd, *J* = 238.6, 12.8 Hz), 138.07 (dd, *J* = 9.5, 2.5 Hz), 127.36 (q, *J* = 3.7 Hz), 125.03 (q, *J* = 270.8 Hz), 121.29 (q, *J* = 32.4 Hz), 117.60 (d, *J* = 17.2 Hz), 116.13, 114.02 (dd, *J* = 5.7, 3.1 Hz), 106.88 (d, *J* = 21.8 Hz), 78.11, 49.86, 31.19, 30.78. ^{19}F NMR (376 MHz, DMSO-d_6) δ -59.82, -137.83 (ddd, J = 23.1, 13.6, 9.5 Hz), -148.33 (dddd, J = 22.5, 11.1, 7.5, 3.9 Hz). LC-MS (ESI): *m/z* 401.31 $[M+H]^+$, 442.39 $[M+H+41]^+$.

4.2.12. Cyclohexyl series (**VI**)

4.2.12.1.
1-(4-Cyano-3-fluorophenyl)-3-(trans-4-(4-(trifluoromethyl)phenoxy)cyclohexyl)urea (**5-VI**)

Prepared in essentially the same way as **4-VI**. White crystalline solid (100 mg, 47%); mp 226.0-228.0 ºC (EtOAc). ^{1}H NMR (400 MHz, DMSO-d_6) δ 9.08 (s, 1H), 7.73 – 7.54 (m, 4H), 7.19 – 7.06 (m, 3H), 6.49 (d, *J* = 7.5 Hz, 1H), 4.45 (ddd, *J* = 13.5, 9.5, 3.8 Hz, 1H), 3.59 – 3.47 (m, 1H), 2.04 (d, *J* = 10.0 Hz, 2H), 2.01 – 1.79 (m, 2H), 1.62 – 1.26 (m, 4H). ^{1}H NMR (400 MHz, DMSO-d_6) δ 9.08 (s, 1H), 7.68 (t, *J* = 8.2 Hz, 1H), 7.65 (d, *J* = 1.9 Hz, 1H), 7.59 (d, *J* = 8.7 Hz, 2H), 7.15 (dd, *J* = 8.7, 1.8 Hz, 1H), 7.11 (d, *J* = 8.6 Hz, 2H), 6.49 (d, *J* = 7.5 Hz, 1H), 4.45 (ddd, *J* = 13.5, 9.5, 3.8 Hz, 1H), 3.59 – 3.48 (m, 1H), 2.04 (d, *J* = 10.0 Hz, 2H), 2.01 – 1.79 (m, 2H), 1.62 – 1.26 (m, 4H). ^{13}C NMR (100 MHz, DMSO-d_6) δ 163.72 (d, *J* = 251.2 Hz), 160.71 (d, *J* = 1.2 Hz), 154.10, 147.68 (d, *J* = 12.1 Hz), 134.42 (d, *J* = 1.9 Hz), 127.36 (q, *J* = 3.6 Hz), 125.01 (q, *J* = 270.8 Hz), 121.27 (q, *J* = 32.0 Hz), 116.26, 115.12, 114.18 (d, *J* = 2.1 Hz), 104.25 (d, *J* = 24.9 Hz), 91.14 (d, *J* = 15.6 Hz), 74.79, 47.73, 30.11, 29.89. ^{19}F NMR (376 MHz, DMSO-d_6) δ -59.83, -107.34 (dd, *J* = 12.8, 7.8 Hz). LC-MS (ESI): *m/z* 421.95$[M+H]^+$, 463.03 $[M+H+41]^+$.

4.2.12.2.

1-(5-Cyano-2-fluorophenyl)-3-(trans-4-(4-(trifluoromethyl)phenoxy)cyclohexyl)urea (**6-VI**)

Prepared in essentially the same way as **4-VI**. Off white solid (110 mg, 52%); mp 234.6-237.0 ºC (EtOAc). ^{1}H NMR (400 MHz, DMSO-d_6) δ 8.56 (d, *J* = 7.8 Hz, 1H), 8.53 (d, *J* = 2.8 Hz, 1H), 7.60 (d, *J* = 8.7 Hz, 2H), 7.45 – 7.36 (m, 2H), 7.12 (d, *J* = 8.6 Hz, 2H), 6.77 (d, *J* = 7.4 Hz, 1H), 4.48 (ddd, *J* = 13.4, 9.4, 3.7 Hz, 1H), 3.65 – 3.39 (m, 1H), 2.12 – 1.98 (m, 2H), 1.99 – 1.87 (m, 2H), 1.51 (td, *J* = 12.5, 2.9 Hz, 2H), 1.36 (td, *J* = 12.7, 2.8 Hz, 2H). ^{13}C NMR (100 MHz, DMSO-d_6) δ 160.72 (d, *J* = 1.1 Hz), 154.26, 154.01 (d, *J* = 250.5 Hz), 130.18 (d, *J* = 11.5 Hz), 127.36 (q, *J* = 3.6 Hz), 126.20 (d, *J* = 8.6 Hz), 125.01 (q, *J* = 270.8 Hz), 122.92 (d, *J* = 3.8 Hz), 121.27 (q, *J* = 31.9 Hz), 118.90, 116.94 (d, *J* = 20.9 Hz), 116.28, 107.99 (d, *J* = 3.4 Hz), 74.64, 47.54, 30.05, 29.68. ^{19}F NMR (376 MHz, DMSO-d_6) δ -59.81, -121.67. LC-MS (ESI): *m/z* 422.02$[M+H]^+$, 463.23 $[M+H+41]^+$.

4.2.12.3.

1-(5-Fluoro-2-methylphenyl)-3-(trans-4-(4-(trifluoromethyl)phenoxy)cyclohexyl)urea (**7-VI**)

Prepared in essentially the same way as **7-V**. White solid (80 mg, 39%); mp 238.2-239.8 ºC (EtOAc). ^{1}H NMR (400 MHz, DMSO-d_6) δ 7.88 (dd, *J* = 12.6, 2.7 Hz, 1H), 7.65 (s, 1H), 7.60 (d, *J* = 8.7 Hz, 2H), 7.12 (d, *J* = 8.8 Hz, 2H), 7.08 (d, *J* = 7.5 Hz, 1H), 6.77 (d, *J* = 7.4 Hz, 1H), 6.61 (td, *J* = 8.3, 2.8 Hz, 1H), 4.48 (ddd, *J* = 13.4, 9.5, 3.7 Hz, 1H), 3.69 – 3.47 (m, 1H), 2.13 (s, 2H), 2.12 – 2.00 (m, 2H), 1.95 (dd, *J* = 12.9, 3.0 Hz, 2H), 1.50 (td, *J* = 12.5, 2.8 Hz, 2H), 1.35 (td, *J* = 12.7, 2.7 Hz, 2H). ^{13}C NMR (100 MHz, DMSO-d_6) δ 161.08 (d, *J* = 237.4 Hz), 160.75 (d, *J* = 1.2 Hz), 154.80, 140.22 (d, *J* = 11.8 Hz), 131.30 (d, *J* = 9.5 Hz), 127.36 (q, *J* = 3.7 Hz), 125.02 (q, *J* = 270.9 Hz), 121.27 (q, *J* = 32.1 Hz), 121.15 (d, *J* = 2.7 Hz), 116.28, 107.52 (d, *J* = 21.0 Hz), 105.78 (d, *J* = 27.3 Hz), 74.83, 47.59, 30.31, 29.90, 17.64. ^{19}F NMR (376 MHz, DMSO-d_6) δ -59.81, -115.96 (dd, *J* = 13.2, 6.7 Hz). LC-MS (ESI): *m/z* 410.97$[M+H]^+$, 452.05 $[M+H+41]^+$.

4.2.12.4.

1-(4-Cyano-2-fluorophenyl)-3-(trans-4-(4-(trifluoromethyl)phenoxy)cyclohexyl)urea (**8-VI**)

Prepared in essentially the same way as **4-VI**. White solid (100 mg, 47%); mp 221.6-223.6 ºC (EtOAc). ^{1}H NMR (400 MHz, DMSO-d_6) δ 8.66 (d, *J* = 2.0 Hz, 1H), 8.38 (t, *J* = 8.4 Hz, 1H), 7.77 (dd, *J* = 11.5, 1.8 Hz, 1H), 7.60 (d, *J* = 8.7 Hz, 2H), 7.57 – 7.50 (m, 1H), 7.11 (d, *J* = 8.7 Hz, 2H), 6.87 (d, *J* = 7.4 Hz, 1H), 4.48 (ddd, *J* = 13.2, 9.3, 3.6 Hz, 1H), 3.61 – 3.49 (m, 1H), 2.15 – 1.99 (m, 2H), 1.94 (dd, *J* = 12.9, 3.4 Hz, 2H), 1.61 – 1.40 (m, 2H), 1.35 (dt, *J* = 12.9, 6.6 Hz, 2H). ^{13}C NMR (100 MHz, DMSO-d_6) δ 160.72 (d, *J* = 1.1 Hz),

153.90, 150.46 (d, *J* = 243.0 Hz), 134.09 (d, *J* = 10.0 Hz), 130.12 (d, *J* = 3.2 Hz), 127.36 (q, *J* = 3.8 Hz), 125.01 (d, *J* = 271.0 Hz), 121.27 (d, *J* = 32.0 Hz), 119.44 (d, *J* = 2.8 Hz), 118.99 (d, *J* = 22.9 Hz), 118.77 (d, *J* = 2.6 Hz), 116.27, 102.60 (d, *J* = 9.5 Hz), 74.62, 47.52, 30.00, 29.65. ^{19}F NMR (376 MHz, DMSO-d_6) δ -59.82, -129.13. LC-MS (ESI): *m/z* 422.1 $[M+H]^+$, 463.1 $[M+H+41]^+$.

4.2.12.5.
1-(3-Cyano-5-fluorophenyl)-3-(trans-4-(4-(trifluoromethyl)phenoxy)cyclohexyl)urea (**9-VI**)

Prepared in essentially the same way as **4-VI**. Pinky solid (105 mg, 50%); mp 219.8-222.0 ºC (EtOAc). ^{1}H NMR (400 MHz, DMSO-d_6) δ 8.62 (s, 1H), 7.90 (dd, *J* = 5.7, 2.7 Hz, 1H), 7.64 – 7.57 (m, 1H), 7.59 (d, *J* = 8.7 Hz, 2H), 7.37 (t, *J* = 9.1 Hz, 1H), 7.11 (d, *J* = 8.7 Hz, 2H), 6.32 (d, *J* = 7.6 Hz, 1H), 4.44 (ddd, *J* = 13.6, 9.5, 3.8 Hz, 1H), 3.58 – 3.46 (m, 1H), 2.09 – 1.98 (m, 2H), 1.96 – 1.88 (m, 2H), 1.59 – 1.25 (m, 4H). ^{13}C NMR (100 MHz, DMSO-d_6) δ 160.73 (d, *J* = 1.2 Hz), 157.36 (d, *J* = 249.4 Hz), 154.75, 138.14 (d, *J* = 2.7 Hz), 127.36 (q, *J* = 3.6 Hz), 125.18 (d, *J* = 7.7 Hz), 125.01 (q, *J* = 270.9 Hz), 121.33, 121.26 (q, *J* = 32.1 Hz), 117.26 (d, *J* = 20.4 Hz), 116.27, 114.65, 100.09 (d, *J* = 16.0 Hz), 74.86, 47.70, 30.28, 29.96. ^{19}F NMR (376 MHz, DMSO-d_6) δ -59.82, -118.72 (m). LC-MS (ESI): *m/z* 422.22 $[M+H]^+$, 463.23 $[M+H+41]^+$.

4.2.12.6. 1-(3,4-Difluorophenyl)-3-(trans-4-(4-(trifluoromethyl)phenoxy)cyclohexyl)urea (**10-VI**)

Prepared in essentially the same way as **7-V**. White solid (68 mg, 33%); mp 228.2-229.8 ºC (EtOAc). ^{1}H NMR (400 MHz, DMSO-d_6) δ 8.49 (s, 1H), 7.63 – 7.57 (m, 1H), 7.60 (d, *J* = 8.7 Hz, 2H), 7.24 (dd, *J* = 19.7, 9.3 Hz, 1H), 7.11 (d, *J* = 8.6 Hz, 2H), 7.03 – 6.92 (m, 1H), 6.19 (d, *J* = 7.6 Hz, 1H), 4.44 (ddd, *J* = 13.6, 9.5, 3.7 Hz, 1H), 3.57 – 3.46 (m, 1H), 2.16 – 1.94 (m, 2H), 1.94 – 1.79 (m, 2H), 1.59 – 1.25 (m, 4H). ^{13}C NMR (100 MHz, DMSO-d_6) δ 160.73 (d, *J* = 1.2 Hz), 154.79, 149.51 (dd, *J* = 241.8, 13.1 Hz), 144.32 (dd, *J* = 238.6, 12.8 Hz), 138.10 (dd, *J* = 9.5, 2.5 Hz), 127.36 (q, *J* = 3.8 Hz), 125.01 (q, *J* = 270.7 Hz), 121.26 (q, *J* = 32.1 Hz), 117.62 (d, *J* = 16.8 Hz), 116.26, 113.88 (dd, *J* = 5.7, 3.2 Hz), 106.75 (d, *J* = 21.9 Hz), 74.87, 47.60, 30.33, 29.96. ^{19}F NMR (376 MHz, DMSO-d_6) δ -59.82, -137.77 (ddd, *J* = 23.1, 13.6, 9.5 Hz), -148.40 (dddd, *J* = 22.4, 11.0, 7.5, 3.8 Hz). LC-MS (ESI): *m/z* 415.21 $[M+H]^+$, 456.22 $[M+H+41]^+$.

4.2.12.7. 1-(2,3-Difluorophenyl)-3-(trans-4-(4-(trifluoromethyl)phenoxy)cyclohexyl)urea (**11-VI**)

Prepared in essentially the same way as **7-V**. Off white solid (90 mg, 43%); mp 227.3-229.9 ºC (EtOAc). ^{1}H NMR (400 MHz, DMSO-d_6) δ 8.69 (s, 1H), 7.60 (d, *J* = 8.7 Hz, 2H), 7.11 (d, *J* = 8.6 Hz, 2H), 7.10 – 7.05 (m, 1H), 6.65 (tt, *J* = 9.4, 2.3 Hz, 1H), 6.31 (d, *J* = 7.6 Hz, 1H), 4.52 – 4.37 (m, 1H), 3.62 – 3.42 (m, 1H), 2.16 – 1.94 (m, 2H), 1.91 (dd, *J* = 12.9, 3.2 Hz, 2H), 1.59 – 1.26 (m, 4H). ^{13}C NMR (100 MHz, DMSO-d_6) δ 163.04 (dd, *J* = 241.6, 15.8 Hz), 160.73 (d, *J* = 1.0 Hz), 154.49, 127.36 (q, *J* = 3.9 Hz), 125.01 (q, *J* = 270.9 Hz), 121.26 (q, *J* = 32.1 Hz), 120.85 (d, *J* = 6.6 Hz), 116.27, 100.62 (d, *J* = 29.3 Hz), 100.62 (d, *J* = 12.4 Hz), 96.27 (t, *J* = 26.3 Hz), 74.85, 47.65, 30.24, 29.95. ^{19}F NMR (376 MHz, DMSO-d_6) δ -59.82, -110.01 (d, *J* = 9.5 Hz), -110.03 (d, *J* = 9.5 Hz). LC-MS (ESI): *m/z* 415.01 $[M+H]^+$, 456.08 $[M+H+41]^+$.

4.2.13. Pyrimidine series (**py**)

4.2.13.1.1-(3-Cyano-5-(trifluoromethyl)phenyl)-3-(5-(4-(trifluoromethyl)phenoxy)pyrimidin-2-yl)urea (**1-py**)

Prepared in essentially the same way as **4-VI**. White solid (30 mg, 13%); mp 263.5-265.5 ºC (EtOAc). ^{1}H NMR (400 MHz, DMSO-d_6) δ 11.83 (s, 1H), 10.65 (s, 1H), 8.66 (d, *J* = 3.0 Hz, 2H), 8.38 (d, *J* = 13.9 Hz, 2H), 7.96 (s, 1H), 7.76 (d, *J* = 6.5 Hz, 2H), 7.30 (d, *J* = 6.3 Hz, 2H). ^{13}C NMR (100 MHz, DMSO-d_6) δ 160.59 (d, *J* = 0.8 Hz), 154.70, 151.99, 151.13, 145.44, 140.98, 131.34 (q, *J* = 32.7 Hz), 128.09 (q, *J* = 3.9 Hz), 126.45, 124.60 (q, *J* = 271.4 Hz), 124.55 (q, *J* = 31.9 Hz), 124.53 (q, *J* = 269.1 Hz), 123.24 (d, *J* = 4.4 Hz), 120.22 (d, *J* = 4.3 Hz), 118.18, 117.87, 113.50. ^{19}F NMR (376 MHz, DMSO-d_6) δ -60.31, -61.68. LC-MS (ESI): *m/z* 467.99 $[M+H]^+$, 509.06 $[M+H+41]^+$.

4.2.13.2.1-(5-(4-(Trifluoromethyl)phenoxy)pyrimidin-2-yl)-3-(3-(trifluoromethyl)phenyl)urea (**2-py**)

Prepared in essentially the same way as **7-V**. White solid (55 mg, 31%); mp 232.5-234.8 ºC (EtOAc). ^{1}H NMR (400 MHz, DMSO-d_6) δ 11.49 (s, 1H), 10.45 (s, 1H), 8.67 (s, 2H), 8.07 (s, 1H), 7.82 (d, *J* = 8.2 Hz, 1H), 7.75 (d, *J* = 8.7 Hz, 2H), 7.55 (t, *J* = 8.0 Hz, 1H), 7.38 (d, *J* = 7.7 Hz, 1H), 7.29 (d, *J* = 8.6 Hz, 2H). ^{13}C NMR (100 MHz, DMSO-d_6) δ 160.75 (d, *J* = 1.2 Hz), 155.01, 151.89, 151.35, 145.11, 139.89, 130.44, 130.08 (d, *J* = 31.5 Hz), 128.05 (q, *J* = 3.7 Hz), 124.62 (q, *J* = 271.4 Hz), 124.57 (q, *J* = 272.2 Hz), 124.41 (q, *J* = 32.2 Hz), 123.48 (d, *J* = 0.9 Hz), 119.76 (q, *J* = 4.0 Hz), 117.98, 115.84 (q, *J* = 4.1 Hz). ^{19}F NMR (376 MHz, DMSO-d_6) δ -60.27, -61.22. LC-MS (ESI): *m/z* 442.99 $[M+H]^+$.

4.2.13.3. 1-(3-Cyanophenyl)-3-(5-(4-(trifluoromethyl)phenoxy)pyrimidin-2-yl)urea (**3-py**)

Prepared in essentially the same way as **7-V**. White solid (20 mg, 17%); mp 260.2-261.5 ºC (EtOAc). ^{1}H NMR (400 MHz, DMSO-d_6) δ 11.52 (s, 1H), 10.49 (s, 1H), 8.66 (s, 2H), 8.09 (s, 1H), 7.91 (d, *J* = 8.0 Hz, 1H), 7.75 (d, *J* = 8.6 Hz, 2H), 7.59 – 7.41 (m, 2H), 7.29 (d, *J* = 8.5 Hz, 2H). ^{13}C NMR (100 MHz, DMSO-d_6) δ 160.69 (d, *J* = 0.9 Hz), 154.94, 151.85, 151.26, 145.17, 139.96, 130.71, 128.06 (d, *J* = 3.8 Hz), 126.90, 124.62 (d, *J* = 271.5 Hz), 124.45 (d, *J* = 32.3 Hz), 124.37, 122.53, 119.13, 118.02, 112.15. ^{19}F NMR (376 MHz, DMSO-d_6) δ -60.28. LC-MS (ESI): *m/z* 399.99 $[M+H]^+$, 441.07 $[M+H+41]^+$.

4.2.13.4.
1-(3-Cyano-5-fluorophenyl)-3-(5-(4-(trifluoromethyl)phenoxy)pyrimidin-2-yl)urea (**4-py**)

Prepared in essentially the same way as **4-VI**. White solid (20 mg, 19%); mp 267.5-270.0 ºC (EtOAc). ^{1}H NMR (400 MHz, DMSO-d_6) δ 11.73 (s, 1H), 10.58 (s, 1H), 8.64 (s, 2H), 7.95 (d, *J* = 10.9 Hz, 1H), 7.90 (s, 1H), 7.75 (d, *J* = 6.9 Hz, 2H), 7.48 (d, *J* = 7.4 Hz, 1H), 7.29 (d, *J* = 7.0 Hz, 2H). ^{13}C NMR (100 MHz, DMSO-d_6) δ 162.38 (d, *J* = 244.4 Hz), 160.58 (d, *J* = 1.8 Hz), 154.73, 151.83, 151.11, 145.39, 141.94 (d, *J* = 12.0 Hz), 128.08 (q, *J* = 3.6 Hz), 124.60 (q, *J* = 271.2 Hz), 124.55 (q, *J* = 32.2 Hz), 119.27 (d, *J* = 3.4 Hz), 118.17, 118.07 (d, *J* = 3.2 Hz), 113.49 (d, *J* = 25.5 Hz), 113.30 (d, *J* = 12.1 Hz), 111.43 (d, *J* = 26.6 Hz). ^{19}F NMR (376 MHz, DMSO-d_6) δ -60.30, -109.35 (dd, *J* = 11.3, 8.4 Hz). LC-MS (ESI): *m/z* 418.05 $[M+H]^+$, 459.13 $[M+H+41]^+$.

4.2.13.5.
1-(5-Fluoro-2-methylphenyl)-3-(5-(4-(trifluoromethyl)phenoxy)pyrimidin-2-yl)urea (**7-py**)

Prepared in essentially the same way as **7-V**. White crystalline solid (30 mg, 7%); mp 224.2-226.5 ºC (EtOAc). ^{1}H NMR (400 MHz, DMSO-d_6) δ 11.35 (s, 1H), 10.51 (s, 1H), 8.71 (s, 2H), 7.99 (dd, *J* = 11.9, 2.3 Hz, 1H), 7.74 (d, *J* = 8.6 Hz, 2H), 7.27 (d, *J* = 8.5 Hz, 2H), 7.25 – 7.19 (m, 1H), 6.78 (td, *J* = 8.3, 2.4 Hz, 1H), 2.29 (s, 3H). ^{13}C NMR (100 MHz, DMSO-d_6) δ 161.01 (d, *J* = 238.4 Hz), 160.91 (d, *J* = 1.3 Hz), 155.15, 151.73, 151.60, 144.87, 138.87 (d, *J* = 11.5 Hz), 131.61 (d, *J* = 9.3 Hz), 128.00 (q, *J* = 4.0 Hz), 124.63 (q, *J* = 271.5 Hz), 124.28 (q, *J* = 32.2 Hz), 122.78 (d, *J* = 2.9 Hz), 117.74, 109.37 (d, *J* = 21.1 Hz), 106.85 (d, *J* = 27.2 Hz), 17.86. ^{19}F NMR (376 MHz, DMSO-d_6) δ -60.24, -115.62 (m). LC-MS (ESI): *m/z* 407.14 $[M+H]^+$, 448.21 $[M+H+41]^+$.

4.2.13.6. 1-(3,4-Difluorophenyl)-3-(5-(4-(trifluoromethyl)phenoxy)pyrimidin-2-yl)urea (**10-py**)

Prepared in essentially the same way as **7-V**. White solid (40 mg, 39%); mp 224.8-226.2 ºC (EtOAc). ^{1}H NMR (400 MHz, DMSO-d_6) δ 11.36 (s, 1H), 10.41 (s, 1H), 8.64 (s, 2H),

7.83 – 7.77 (m, 1H), 7.75 (d, *J* = 8.9 Hz, 2H), 7.43 – 7.30 (m, 2H), 7.28 (d, *J* = 8.6 Hz, 2H). ^{13}C NMR (100 MHz, DMSO-d_6) δ 160.73 (d, *J* = 1.3 Hz), 155.01, 151.80, 151.29, 149.55 (dd, *J* = 243.3, 13.4 Hz), 145.60 (dd, *J* = 241.0, 12.6 Hz), 145.06, 136.09 (dd, *J* = 9.2, 2.9 Hz), 128.03 (q, *J* = 3.7 Hz), 124.61 (d, *J* = 271.6 Hz), 124.41 (d, *J* = 32.3 Hz), 117.96, 117.90 (d, *J* = 17.1 Hz), 116.06 (d, *J* = 2.3 Hz), 108.89 (d, *J* = 21.6 Hz). ^{19}F NMR (376 MHz, DMSO-d_6) δ -60.30, -137.45 (m), -145.60 (m). LC-MS (ESI): *m/z* 411.04 $[M+H]^+$, 452.12 $[M+H+41]^+$.

4.3 Biology

4.3.1 Plasmids and Ternary complex assay. The dual luciferase expression vector and other plasmids used for these studies are described in [27]. The dual luciferase surrogate eIF2α phosphorylation assay, has been described elsewhere [9]. Briefly, a dual Renilla and Firefly luciferase mammalian reporter vector that transcribes both mRNAs from the same bi-directional enhancer/promoter complex was utilized for generation of surrogate eIF2α phosphorylation assay [27]. Both mRNAs contain the same 90 nucleotide plasmid derived 5'UTR. In addition, 5'UTR of the Firefly luciferase ORF is fused in-frame to the 267 nucleotide ATF-4 5'UTR [9].

4.3.2 Dual luciferase reporter (DLR) assay. Cells expressing firefly and renilla luciferases were assayed with a dual glow luciferase assay kit, per manufacturer's instruction (Promega Inc., Madison, WI). The data calculations were carried out as the ratio of firefly to renilla luciferase signal [27]. Dose-response curves were obtained, and triplicate data points were fitted to the logistical sigmoidal model using nonlinear least-squares regression performed in GraphPad Prism 6.

4.3.3 Cell lines and siRNA transfection. Stable cell lines utilized in this study are generated as described elsewhere [9,29]. Briefly, cells were seeded at the density of 10^5 in 60-mm dish and transfected one day later using the Lipofectamine 2000 (Invitrogen). For

selection of stable cell lines, transfected cells were transferred to 100-mm plates and selected with appropriate antibiotics [9]. siRNA knockdown was carried out in 96-well plates by reverse transfection as previously described [9].

4.3.4 Western blotting. Cells cultured under recommended media conditions, were plated and maintained in serum-containing media without antibiotics in 14-cm plates (Nunc) until reaching 70% confluence. Cells were then treated with compounds for 6 hours, washed with cold PBS once, and lysed with M-PER Mammalian Protein Extraction Reagent (Pierce) for 30 minutes on ice. The cell lysates were centrifuged at 12,000 RPM for 15 min and the supernatants were transferred to fresh tubes and the concentrations were determined by BCA (Pierce). Equal amount of proteins were mixed with Laemmli Sample Buffer, heated at 100^{o}C for 5 min and separated by SDS-PAGE and probed with anti-phosphoserine-51-eIF2α (Phos-eIF2α), anti-total eIF2α-specific antibodies (Total-eIF2α) (Biosource International, Hopkinton, MA), anti-CHOP, anti-cyclin D1 or anti-actin (Santa Cruz Biotechnology, CA) essentially as described [35].

4.3.5 Cell Growth Inhibition Assay. Cells were seeded in 96-well plates and maintained for 5 days in the presence of 0.5 to 20 μM of individual compound, and cell proliferation was measured by the sulforhodamine B (SRB) assay as described [36]: briefly, at the end of a 5-day treatment, cells were fixed in 10% cold trichloroacetic acid. Cell number was estimated by measuring the remaining bound dye of sulforhodamine B after washing. The percentage of growth was calculated by using the equation: 100× $[(T-T_0)/(C-T_0)]$, where T and C represent the absorbance in treated and control cultures at

Day 5, and T_0 at time zero, respectively. If T is less than T_0, cell death has occurred and can be calculated from $100\times [(T-T_0)/T_0]$.

REFERENCES

[1] J. Igarashi, M. Murase, A. Iizuka, F. Pichierri, M. Martinkova, T. Shimizu, Elucidation of the heme binding site of heme-regulated eukaryotic initiation factor 2α kinase and the role of the regulatory motif in heme sensing by spectroscopic and catalytic studies of mutant proteins, J. Biol. Chem. 283 (2008) 18782–18791.

[2] J. Igarashi, T. Sasaki, N. Kobayashi, S. Yoshioka, M. Matsushita, T. Shimizu, Autophosphorylation of heme-regulated eukaryotic initiation factor 2a kinase and the role of the modification in catalysis, FEBS J. 278 (2011) 918–928.

[3] C. de la Parra, B.A. Walters, P. Geter, R.J. Schneider, Translation initiation factors and their relevance in cancer, Curr. Opin. Genet. Dev. 48 (2018) 82–88.

[4] A.-P. Han, M.D. Fleming, J.-J. Chen, Heme-regulated eIF2α kinase modifies the phenotypic severity of murine models of erythropoietic protoporphyria and β-thalassemia, J. Clin. Invest. 115 (2005) 1562-1570.

[5] R.N.V.S. Suragani, R.S. Zachariah, J.G. Velazquez, S. Liu, C.-W. Sun, T.M. Townes, J.-J. Chen, Heme-regulated eIF2α kinase activated Atf4 signaling pathway in oxidative stress and erythropoiesis, Blood, 119 (2012) 5276-5284.

[6] J. Igarashi, A. Sato, T. Kitagawa, T. Yoshimura, S. Yamauchi, I. Sagami, T. Shimizu, Activation of heme-regulated eukaryotic initiation factor 2α kinase by nitric oxide is

induced by the formation of a five-coordinate NO-heme complex, J. Biol. Chem. 279 (2004) 15752–15762.

[7] S.K. Berwal, V. Bhatia, A. Bendre, C.G. Suresh, S. Chatterjee, J. K. Pal, Activation of HRI is mediated by Hsp90 during stress through modulation of the HRI-Hsp90 complex, Int. J. Biol. Macromol. 118 (2018) 1604-1613.

[8] N. Burwick, B.H. Aktas, The eIF2-alpha kinase HRI: a potential target beyond the red blood cell, Expert Opin. Ther. Targets, 21 (2017) 1171-1177.

[9] T. Chen, D. Ozel, Y. Qiao, F. Harbinski, L. Chen, S. Denoyelle, X. He, N. Zvereva, J.G. Supko, M. Chorev, J.A. Halperin, B.H. Aktas, Chemical genetics identify eIF2α kinase heme-regulated inhibitor as an anticancer target, Nat. Chem. Biol. 7 (2011) 610−616.

[10] S. Denoyelle, T. Chen, L. Chen, Y. Wang, E. Klosi, J.A. Halperin, B.H. Aktas, M. Chorev, In vitro inhibition of translation initiation by N,N'-diarylureas – potential anti-cancer agents, Bioorg. Med. Chem. Lett. 22 (2012) 402−409.

[11] T. Chen, K. Takrouri, S. Hee-Hwang, S. Rana, R. Yefidoff-Freedman, J. Halperin, A. Natarajan, C. Morisseau, B. Hammock, M. Chorev, B.H. Aktas, Explorations of substituted urea functionality for the discovery of new activators of the heme-regulated inhibitor kinase, J. Med. Chem. 56 (2013) 9457−9470.

[12] R. Yefidoff-Freedman, J. Fan, Y. Lu, Q. Zhang, G.R.R.M. dos Santos, S. Rana, J.I. Contreras, R. Sahoo, D. Wang, J. Young, K.L. Dias-Teixeira, J. Halperin, B. Hammock, A. Natarajan, P. Wang, M. Chorev, B.H. Aktas, Development of 1-((1,4-trans)-4-aryloxycyclohexyl)-3-arylurea activators of the Heme Regulated

Inhibitor as selective activators of eIF2α phosphorylation arm of the integrated endoplasmic reticulum stress response, J. Med. Chem. 60 (2017) 5392−5406.

[13] M. Zarei, E. Barroso, R. Leiva, M. Barniol-Xicota, E. Pujol, C. Escolano, S. Vázquez, X. Palomer, V. Pardo, Á. González-Rodríguez, Á.M. Valverde, T. Quesada-López, F. Villarroya, W. Wahli, M. Vázquez-Carrera, Heme-Regulated eIF2α Kinase modulates hepatic FGF21 and is activated by PPARβ/δ deficiency, Diabetes, (2016) db160155.

[14] M. Zarei, E. Barroso, X. Palomer, J. Dai, P. Rada, T. Quesada-López, J.C. Escolà-Gil, L. Cedó, M.R. Zali, M. Molaei, R. Dabiri, S. Vázquez, E. Pujol, Á.M. Valverde, F. Villarroya, Y. Liu, W. Wahli, M. Vázquez-Carrera, Hepatic regulation of VLDL receptor by PPARβ/δ and FGF21 modulates non-alcoholic fatty liver disease, Mol. Metab. 8 (2018) 117-131.

[15] W. Bahnan, J.C. Boucher, P. Gayle, N. Shrestha, M. Rosen, B. Aktas, R.D. Adkins, A.L. Ager, W. Khan, K. Schesser, The eIF2α kinase heme-regulated inhibitor protects the host from infection by regulating intracellular pathogen trafficking, Infect. Immun. 86 (2018) e00707-17.

[16] F.C. Machado, C.H. Franco, J.V. dos Santos Neto, K.L. Dias-Teixeira, C.B. Moraes, U.G. Lopes, B.H. Aktas, S. Schenkman, Identification of di-substituted ureas that prevent growth of trypanosomes through inhibition of translation initiation, Sci. Rep. 8 (2018) 4857.

[17] N. Burwick, M. Y. Zhang, P. de la Puentec, A.K. Azabc, T.S. Hyuna, M. Ruiz-Gutierreze, M. Sanchez-Bonilla, T. Nakamura, J.J. Delrow, V.L. MacKay, A.

Shimamura, The eIF2-alpha kinase HRI is a novel therapeutic target in multiple myeloma, Leuk. Res. 55 (2017) 23-32.

[18] B.H. Aktas, Y. Qiao, E. Ozdelen, R. Schubert, S. Sevinc, F. Harbinski, L. Grubissich, S. Singer, J.A. Halperin, Small-molecule targeting of translation initiation for cancer therapy, Oncotarget, 4 (2013) 1606-1617.

[19] B.H. Aktas, P. Bordelois, S. Peker, S. Merajver, J.A. Halperin, Depletion of eIF2·GTP·Met-tRNAi translation initiation complex up-regulates BRCA1 expression in vitro and in vivo, Oncotarget, 6 (2015) 6902-6914.

[20] T. Shimizu, A. Lengalova, V. Martínek, M. Martínková, Heme: emergent roles of heme in signal transduction, functional regulation and as catalytic centres, Chem. Soc. Rev. 48 (2019) 5624-5657.

[21] C. Sidrauski, A.M. McGeachy, N.T. Ingolia, P. Walter, The small molecule ISRIB reverses the effects of eIF2α phosphorylation on translation and stress granule assembly. eLife, 4 (2015) e05033.

[22] C. Tenkerian, J. Krishnamoorthy, Z. Mounir, U. Kazimierczak, A. Khoutorsky, K.A. Staschke, A.S. Kristof, S. Wang, M. Hatzoglou, A.E. Koromilas, mTORC2 balances AKT activation and eIF2α serine 51 phosphorylation to promote survival under stress, Mol. Cancer Res. 13 (2015) 1377-1388.

[23] L. Wang, B. Popko, R.P. Roos, An enhanced integrated stress response ameliorates mutant SOD1-induced ALS, Hum. Mol. Genet. 23 (2014) 2629-2638.

[24] H.J. Kim, A.R. Raphael, E.S. LaDow, L. McGurk, R.A. Weber, J.Q. Trojanowski, V.M. Lee, S. Finkbeiner, A.D. Gitler, N.M. Bonini, Therapeutic modulation of eIF2α

phosphorylation rescues TDP-43 toxicity in amyotrophic lateral sclerosis disease models, Nat. Genet. 46 (2013) 152-160.

[25] M. Lemieux, J. Popovici-Muller, J. Travins, Z. Cai, D. Cui, D. Zhou, N-Cyclobutyl-imidazopyridine or -pyrazolopyridine carboxamides as TRPV1 antagonists. PCT Int. Appl. WO 2012072512, June 7, 2012.

[26] O. Mitsunobu, The use of diethyl azodicarboxylate and triphenylphosphine in synthesis and transformation of natural products, Synthesis, (1981) 1-28.

[27] Ziegeler, G.; Ming, J.; Koseki, J. C.; Sevinc, S.; Chen, T.; Ergun, S.; Qin, X.; Aktas, B. H. Embryonic lethal abnormal vision-like HuR-dependent mRNA stability regulates post-transcriptional expression of cyclin-dependent kinase inhibitor p27Kip1. J. Biol. Chem. 285 (2010) 15408−15419.

[28] H. Aktas, R. Fluckiger, J.A. Acosta, J.M. Savage, S.S. Palakurthi, J.A. Halperin, Depletion of intracellular Ca^{2+} stores, phosphorylation of eIF2α, and sustained inhibition of translation initiation mediate the anticancer effects of clotrimazole. Proc. Natl. Acad. Sci. U. S. A. 95 (1998) 8280-8285.

[29] H. Bai, T. Chen, J. Ming, H. Sun, P. Cao, D.N. Fusco, R.T. Chung, M. Chorev, Q. Jin, B.H. Aktas, Dual activators of protein kinase R (PKR) and protein kinase R-like kinase PERK identify common and divergent catalytic targets, ChemBioChem, 14 (2013) 1255-1262.

[30] H.C. Shen, B.D. Hammock. Discovery of inhibitors of soluble epoxide hydrolase: A target with multiple potential therapeutic indications, J. Med. Chem. 55 (2012) 1789-1808.

[31] P. Furet, G. Caravatti, V. Guagnano, M. Lang, T. Meyer, J. Schoepfer. Entry into a new class of protein kinase inhibitors by pseudo ring design. Bioorg. Med. Chem. Lett. 18 (2008) 897-900.

[32] V. Guagnano, P. Furet, C. Spanka, V. Bordas, M. Le Douget, C. Stamm, J. Brueggen, M.R. Jensen, C. Schnell, H. Schmid, M. Wartmann, J. Berghausen, P. Drueckes, A. Zimmerlin, D. Bussiere, J. Murray, D.G. Porta. Discovery of 3-(2,6-dichloro-3,5-dimethoxy-phenyl)-1-{6-[4-(4-ethyl-piperazin-1-yl)-phenylamino] -pyrimidin-4-yl}-1-methyl-urea (NVP-BGJ398), a potent and selective inhibitor of the fibroblast growth factor receptor family of receptor tyrosine kinase, J. Med. Chem. 54 (2011) 7066-7083.

[33] B. Kuhn, P. Mohr, M. Stahl. Intramolecular hydrogen bonding in medicinal chemistry. J. Med. Chem. 53 (2010) 2601-2611.

[34] H. Aktas, J.A. Halperin, Translational regulation of gene expression by omega-3 fatty acids, J. Nutr. 134 (2004) 2487S−2491S.

[35] H. Aktas, H. Cai, G.M. Cooper, Ras links growth factor signaling to the cell cycle machinery via regulation of cyclin D1 and the Cdk inhibitor p27KIP1, Mol. Cell. Biol. 17 (1997) 3850-3857.

[36] S.S. Palakurthi, R. Fluckiger, H. Aktas, A.K. Changolkar, A. Shahsafaei, S. Harneit, E. Kilic, J.A. Halperin, Inhibition of translation initiation mediates the anticancer effect of the n-3 polyunsaturated fatty acid eicosapentaenoic acid, Cancer Res. 60 (2000) 2919-2925.

Acknowledgements

This work was supported by NIH/NCI grant #1RO1CA152312 to B.H. Aktas, by the China Scholarship Council grant 201408310035 and Shanghai Science and Technology Committee (STCSM, China) grant 16430723900 both to Q. Zhang, and by the Brazilian National Council for Scientific and Technological Development (CNPq #249194/2013-9) to G.R.R.M. dos Santos.

Author contributions;

BHA, MC, QZ conceived and directed the study, QZ undertook chemical synthesis and characterization of the compounds, RD and GRRMDS planned and carried out biological characterization of compounds, AB resolved the single crystal structure, RYF contributed to trouble shooting the chemical synthesis, JAH contributed to experimental conceptions, All authors contributed to discussion of results, data interpretation, writing and/or editing the manuscript.

Conflict of Interest:

Authors declare no conflict of interest.

Table 1: cLogP and biological activities of the 1-(4-(trifluoromethyl)phenoxycycloalkyl)-3-(phenyl)ureas ((4-CF_3)ΦO*c*AlkΦUs)

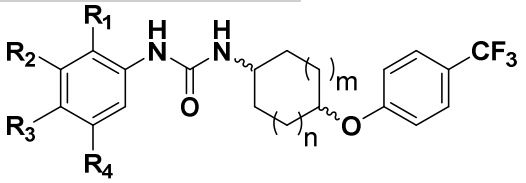

Substituents on the *N*-phenyl				Fold stimulation of ATF-4 Surrogate eIF2α @ 1.25 μM			Fold stimulation of ATF-4 Surrogate eIF2α @ 5 μM			IC_{50}[a] [μM]			cLogP		
R_1	R_2	R_3	R_4	*c*-Hex[b]	*c*-Pent[c]	*c*-But[d]	*c*-Hex[b]	*c*-Pent[c]	*c*-But[d]	*c*-Hex[b]	*c*-Pent[c]	*c*-But[d]	*c*-Hex[b]	*c*-Pent[c]	*c*-But[d]
H	CF_3	H	CN	5.7±1.4	3.1±0.7	4.4±1.1	13.8±1.5	8.3±2.4	10±1.8	0.35±0.1	1.2±0.5	0.9±0.3	6.20	6.08	5.96
				1-VI	1-V	1-IV	1-VI	1-V	1-IV	1-VI	1-V	1-IV	1-VI	1-V	1-IV
						4.3±0.6			8.4±0.5			0.9±0.3			5.96
						1-IVc			1-IVc			1-IVc			1-IVc
H	CF_3	H	H	3.6±1.2	1.2±0.4	2.4±0.6	9.2±1.4	7±0.9	6.5±1.2	0.9±0.5	2.5±0.5	3.4±1	6.41	6.29	6.16
				2-VI	2-V	2-IV	2-VI	2-V	2-IV	2-VI	2-V	2-IV	2-VI	2-V	2-IV
						1.2±0.3			6.2±1.2			2.6±0.4			6.16
						2-IVc			2-IVc			2-IVc			2-IVc
H	CN	H	H	1.9±0.4	0.8±0.2	1.6±0.2	6.1±0.9	1.6±0.2	3.5±0.4	1.6±1	6.5±2.3	4.9±0.9	5.13	5.01	4.78
				3-VI	3-V	3-IV	3-VI	3-V	3-IV	3-VI	3-V	3-IV	3-VI	3-V	3-IV
						1.1±0.2			0.9±0.1			>10			4.78
						3-IVc			3-IVc			3-IVc			3-IVc
H	F	H	CN	4.6±0.7	2.4±0.3	2±0.4	9.3±1.3	8±2	5.3±0.6	0.63±0.3	1.9±1.3	2.8±1.3	5.38	5.26	5.03
				4-VI	4-V	4-IV	4-VI	4-V	4-IV	4-VI	4-V	4-IV	4-VI	4-V	4-IV
H	F	CN	H	5.5±0.4			10.4±1			0.46±0.1			5.38		
				5-VI			5-VI			5-VI			5-VI		
F	H	H	CN	1±0.3			1.5±0.5			>10			4.93		
				6-VI			6-VI			6-VI			6-VI		
CH_3	H	H	F	1.8±0.8	1.4±0.1	0.7±0.2	1.5±0.4	1.3±0.4	1.4±0.1	5.3±1.8	8±2.5	>10	5.38	5.26	5.03
				7-VI	7-V	7-IV	7-VI	7-V	7-IV	7-VI	7-V	7-IV	7-VI	7-V	7-IV
F	H	CN	H	2.4±0.4			6.2±1.3			1.4±0.3			4.93		
				8-VI			8-VI			8-VI			8-VI		
H	CN	F	H	3.7±0.8			6.1±1.1			1.4±0.3			5.38		
				9-VI			9-VI			9-VI			9-VI		
H	F	F	H	2.9±0.7	0.9±0.2	2.2±0.5	5.6±1.2	3.5±0.7	4.5±0.4	1.3±0.3	5.2±1.5	5.5±0.7	5.62	5.50	5.27
				10-VI	10-V	10-IV	10-VI	10-V	10-IV	10-VI	10-V	10-IV	10-VI	10-V	10-IV
F	F	H	H	4.7±1		0.8±0.1	9.9±1.3		6.2±2.7	1.6±02		2.3±0.9	5.17		4.82
				11-VI		11-IV	11-VI		11-IV	11-VI		11-IV	11-VI		11-IV

[a] Concentration that inhibits growth of human melanoma CRL-2813 cells by 50% ; [b] *c*-Hex (cyclohexyl, m=1, n=1); [c] *c*-Pent (cyclopentyl, m=0, n=1); [d] *c*-But (cyclobutyl, m=0, n=0)

Highlights:

New eIF2α Kinase Heme-Regulated Inhibitor (HRI) activators with improved druglikeness.

New HRI activators with significantly improved cLogPs and no loss of potencies.

Mechanistic assays confirm they are targeting eIF2α phosphorylation by activating HRI.

These HRI activators are excellent first-in-class preclinical candidates for cancer therapy.

Extensive structure – activity relationship studies complement previous findings.

Declaration of interests

☐ The authors declare that they have no known competing financial interests or personal relationships that could have appeared to influence the work reported in this paper.

☒The authors declare the following financial interests/personal relationships which may be considered as potential competing interests:

BHA, MC and QZ are inventors on a patent application that includes the compounds reported here in.